

# **UNIVERSIDAD DE INVESTIGACIÓN DE TECNOLOGÍA EXPERIMENTAL YACHAY**

**Escuela de Ciencias Físicas y Nanotecnología**

## **TÍTULO: CONTROLLED QUANTUM TELEPORTATION OVER NOISY CHANNELS**

Trabajo de integración curricular presentado como requisito para la obtención  
del título de Físico

**AUTOR:**

Vega Alcívar Andrés Paúl

**TUTOR:**

Ph.D. Svozilík Jiří

Urququí, Julio 2020

**SECRETARÍA GENERAL**  
**(Vicerrectorado Académico/Cancillería)**  
**ESCUELA DE CIENCIAS FÍSICAS Y NANOTECNOLOGÍA**  
**CARRERA DE FÍSICA**  
**ACTA DE DEFENSA No. UITEY-PHY-2020-00014-AD**

A los 17 días del mes de julio de 2020, a las 14:00 horas, de manera virtual mediante videoconferencia, y ante el Tribunal Calificador, integrado por los docentes:

<b>Presidente Tribunal de Defensa</b>	Dr. MEDINA DAGGER, ERNESTO ANTONIO , Ph.D.
<b>Miembro No Tutor</b>	Dr. RAMIREZ VELASQUEZ JOSE MANUEL , Ph.D.
<b>Tutor</b>	Dr. SVOZILIK JIRI , Ph.D.

El(la) señor(ita) estudiante **VEGA ALCIVAR, ANDRES PAUL**, con cédula de identidad No. **0917690364**, de la **ESCUELA DE CIENCIAS FÍSICAS Y NANOTECNOLOGÍA**, de la Carrera de **FÍSICA**, aprobada por el Consejo de Educación Superior (CES), mediante Resolución **RPC-SO-39-No.456-2014**, realiza a través de videoconferencia, la sustentación de su trabajo de titulación denominado: **Controlled Quantum Telleportation Over Noisy Channels**, previa a la obtención del título de **FÍSICO/A**.

El citado trabajo de titulación, fue debidamente aprobado por el(los) docente(s):

<b>Tutor</b>	Dr. SVOZILIK JIRI , Ph.D.
--------------	---------------------------

Y recibió las observaciones de los otros miembros del Tribunal Calificador, las mismas que han sido incorporadas por el(la) estudiante.

Previamente cumplidos los requisitos legales y reglamentarios, el trabajo de titulación fue sustentado por el(la) estudiante y examinado por los miembros del Tribunal Calificador. Escuchada la sustentación del trabajo de titulación a través de videoconferencia, que integró la exposición de el(la) estudiante sobre el contenido de la misma y las preguntas formuladas por los miembros del Tribunal, se califica la sustentación del trabajo de titulación con las siguientes calificaciones:

Tipo	Docente	Calificación
Miembro Tribunal De Defensa	Dr. RAMIREZ VELASQUEZ JOSE MANUEL , Ph.D.	9,3
Presidente Tribunal De Defensa	Dr. MEDINA DAGGER, ERNESTO ANTONIO , Ph.D.	9,0
Tutor	Dr. SVOZILIK JIRI , Ph.D.	9,6

Lo que da un promedio de: **9.3 (Nueve punto Tres)**, sobre 10 (diez), equivalente a: **APROBADO**

Para constancia de lo actuado, firman los miembros del Tribunal Calificador, el/la estudiante y el/la secretario ad-hoc.

*Certifico que en cumplimiento del Decreto Ejecutivo 1017 de 16 de marzo de 2020, la defensa de trabajo de titulación (o examen de grado modalidad teórico práctica) se realizó vía virtual, por lo que las firmas de los miembros del Tribunal de Defensa de Grado, constan en forma digital.*

VEGA ALCIVAR, ANDRES PAUL  
**Estudiante**

Dr. MEDINA DAGGER, ERNESTO ANTONIO , Ph.D.  
**Presidente Tribunal de Defensa**

Dr. SVOZILIK JIRI , Ph.D.  
**Tutor**

Dr. RAMIREZ VELASQUEZ JOSE MANUEL , Ph.D.  
**Miembro No Tutor**

CIFUENTES TAFUR, EVELYN CAROLINA  
**Secretario Ad-hoc**

## **AUTORÍA**

Yo, **ANDRES PAUL VEGA ALCIVAR** , con cédula de identidad 0917690364, declaro que las ideas, juicios, valoraciones, interpretaciones, consultas bibliográficas, definiciones y conceptualizaciones expuestas en el presente trabajo; así cómo, los procedimientos y herramientas utilizadas en la investigación, son de absoluta responsabilidad de el autora del trabajo de integración curricular. Así mismo, me acojo a los reglamentos internos de la Universidad de Investigación de Tecnología Experimental Yachay.

Urququí, Julio 2020.



---

Andrés Paúl Vega Alcívar  
CI: 0917690364



## AUTORIZACIÓN DE PUBLICACIÓN

Yo, **ANDRES PAUL VEGA ALCIVAR**, con cédula de identidad 0917690364, cedo a la Universidad de Tecnología Experimental Yachay, los derechos de publicación de la presente obra, sin que deba haber un reconocimiento económico por este concepto. Declaro además que el texto del presente trabajo de titulación no podrá ser cedido a ninguna empresa editorial para su publicación u otros fines, sin contar previamente con la autorización escrita de la Universidad.

Asimismo, autorizo a la Universidad que realice la digitalización y publicación de este trabajo de integración curricular en el repositorio virtual, de conformidad a lo dispuesto en el Art. 144 de la Ley Orgánica de Educación Superior

Urcuquí, Julio 2020.



---

Andrés Paúl Vega Alcívar

CI: 0917690364

## Abstract

Quantum teleportation (QT) is the principal method of transferring quantum states from one place to another without actually revealing which quantum state is being transferred. This protocol makes use of entangled states shared between the sending and receiving stations, and two bits of classical information. However, in real communication systems which are used to carry the entangled state, a typical noise results in the degradation of the fidelity of teleported states. The protocol of controlled quantum teleportation (CQT) represents an extension to the standard quantum teleportation (SQT) which includes the third entity, so called “controller“, and is based on sharing of a tripartite entangled quantum state. The role of controller is to permit the fidelity of teleported state to be higher than it can be done using only classical resources.

As a typical noise has detrimental effect on the performance of quantum teleportation protocols, In this work, a study of different noisy channels, which can exhibit the Markovian or non-Markovian dynamics is presented. Each noisy channel is characterized by the teleportation fidelity and by the control power.

**Keywords:** Fidelity, entangled states, Master equation, Markovian, Non-Markovian

## Resumen

Teleportación cuántica (TC) es el principal método empleado para transferir estados cuánticos de un lugar a otro sin revelar realmente qué estado cuántico se está transfiriendo. Este protocolo utiliza estados entrelazados compartidos entre las estaciones de envío y recepción, y dos bits de información clásica. Sin embargo, en los sistemas de comunicación reales que se utilizan para transportar el estado enredado, un ruido típico da como resultado la degradación de la fidelidad de los estados teletransportados. El protocolo de teleportación cuántica controlada (TCC) representa una extensión de la teleportación cuántica estandar (TCS) la cual incluye una tercera entidad, llamada "controlador", y se basa en compartir un estado cuántico entrelazado tripartito. El papel del controlador es permitir que la fidelidad del estado teletransportado sea mayor de la que se puede alcanzar empleando unicamente recursos clásicos.

Como un ruido típico tiene un efecto perjudicial en el rendimiento de los protocolos de teletransportación cuántica, en este trabajo, se presenta un estudio de diferentes canales ruidosos, que pueden exhibir la dinámica markoviana o no markoviana. Cada canal ruidoso se caracteriza por la fidelidad de teletransportación y por el poder de control.

**Palabras clave:** Fidelidad, estados entrelazados, ecuación maestra, markoviano, no markoviano

## **Acknowledgements**

"If I have seen further, it is by standing upon the shoulders of giants."

Isaac Newton

I wish to express my deepest gratitude to my thesis advisor, Ph.D Jiří Svozilík who keeps an incredible level of support and patience during the elaboration of this work. Certainly, his attitude and passion for science resulted in very inspiring for me. Without his guidance and persistent help, this work would not have been possible.

I would like to thanks my professors who drop by drop were participants of my progress and discovery of this beautiful world of physics. Their passion for teaching was delightful for me and opened my mind to a new horizon of curiosity. I will carry all of them in my heart.

I am in debt o my parents, whose dedication and unconditional support have always been the fundamental key to achieve my dreams. Finally for everyone of my familiar and friends whom one way or another were there supporting me in every single step, their names may not all be enumerated. I would like to thank all of them.



# Contents

<b>List of Figures</b>	<b>ix</b>
<b>List of Tables</b>	<b>xii</b>
<b>1 Introduction</b>	<b>1</b>
1.1 Standard Quantum Teleportation . . . . .	1
1.2 Controlled Quantum Teleportation . . . . .	3
1.3 Quantum gates and quantum circuits . . . . .	4
1.4 Fidelity as a quantitative description of protocol efficiency . . . . .	6
1.5 Transmission Through Noisy Channels . . . . .	7
1.6 Non-Markovian Dynamics . . . . .	7
<b>2 Results &amp; Discussion</b>	<b>9</b>
2.1 Standard Quantum Teleportation . . . . .	9
2.1.1 Markovian Channel . . . . .	11
2.1.2 Non-Markovian Channel . . . . .	28
2.2 Controlled Quantum Teleportation . . . . .	36
2.2.1 Markovian Channel . . . . .	37
2.2.2 Non-Markovian Channel . . . . .	39
<b>3 Conclusions &amp; Outlook</b>	<b>43</b>
<b>Bibliography</b>	<b>45</b>
<b>Abbreviations</b>	<b>47</b>



# List of Figures

1.1	The basic scheme of quantum teleportation, where the letter A stands for the sending station and B for the receiving stations. The environment is marked as E. The solid lines represent quantum channels and dashed lines classical channels. . . . .	1
1.2	The scheme of the controlled quantum teleportation protocol. The letter A stands for the sending, B for receiving, and C for controller's stations. The environment is marked as E. The solid lines represent quantum channels and dashed lines classical channels. . . . .	4
1.3	QT circuit conformed by the quantum gates CNOT, H, X, and Z. It is based in the Standard quantum teleportation protocol described above in the first section. . . . .	5
2.1	Measurements for the average fidelity vs. the parameter p. Red dashed line points the maximum of the function. . . . .	12
2.2	The SQT Fidelity vs $\theta$ and $\phi$ with the noise $\sigma_z$ introduced in the second qubit. a) Bell's state, b), c), d) Werner states. For all the plots, the values $t = 3, \gamma = 1$ were fixed. . . . .	14
2.3	Contour plot of $\gamma$ and $t$ with the noise $\sigma_z$ in the second qubit. Legends in the graphs show the behavior of $F_{avg}$ . a) Bell's state, b), c), d) Werner states. . . . .	15
2.4	The SQT evolution of $F_{avg}$ vs $\gamma$ . Parameter t is fixed with values for a) t=0, b) t=3, c) t=5, d) t=10 . . .	16
2.5	The SQT Fidelity vs $\theta$ and $\phi$ with the noise $\sigma_x$ introduced in the second qubit. a) Bell's state, b), c), d) Werner states. . . . .	17
2.6	The SQT Fidelity vs $\theta$ and $\phi$ with the noise $\sigma_y$ introduced in the second qubit. a) Bell's state, b), c), d) Werner states. . . . .	19
2.7	The SQT Fidelity vs $\theta$ and $\phi$ with the noise $\sigma_z$ introduced in the first and second qubit. a) Bell's state, b), c), d) Werner states. Parameter $t = 3$ , and $\gamma = 1$ were fixed for all the plots . . . . .	20
2.8	SQT Contour plot of $\gamma$ and t with noise $\sigma_z$ over both qubits. Legends in graphs show the $F_{avg}$ . a) Bell's state, b), c), d) Werner states. . . . .	21
2.9	The SQT $F_{avg}$ and $\gamma$ through time with noise $\sigma_z$ acting over both qubits. For the differents plots the value for $t$ was fixed as: a) t=0, b) t=3, c) t=5, d) t=10 . . . . .	22
2.10	The SQT Fidelity vs. $\theta$ and $\phi$ , with $\sigma_x$ noise acting over both qubits. a) Bell's state, b), c), d) Werner states. Values of $t = 3$ , and $\gamma = 1$ were fixed for all the plots. . . . .	23
2.11	Contour plots of $\gamma$ and $t$ with noise $\sigma_z$ acting over both qubits. a) Bell's state, b), c), d) Werner states. . . . .	24
2.12	The SQT $F_{avg}$ and $\gamma$ paramter through time with noise $\sigma_z$ acting over both qubits. Value of t was fixed for each plot a) t=0, b) t=3, c) t=5, and d) t=10 . . . . .	25
2.13	The SQT Fidelity vs $\theta$ and $\phi$ , with noise $\sigma_z$ and $\sigma_x$ acting in second and third qubit. a) Bell's state, b), c), d) Werner states. In each plot values for $t = 3$ , and $\gamma = 5$ were fixed. . . . .	26
2.14	Contour plots $\gamma$ and $t$ , with noise $\sigma_z$ and $\sigma_x$ acting over two qubits. a) Bell's state, b), c), d) Werner states. . . . .	27



2.15	The SQT $F_{avg}$ and $\gamma$ through time with noise $\sigma_z$ and $\sigma_x$ acting over both qubits. For each plot the value for t was fixed a) $t = 0$ , b) $t = 3$ , c) $t = 5$ , d) $t = 10$ . . . . .	28
2.16	The QT fidelity as a function of the coupling strength $d_c$ . Parameter $\omega = 2$ has been fixed for all the plots.	30
2.17	The QT fidelity as a function of the coupling strength $d_c$ and the environment $d_v$ . The different plots show how is the behavior between $F_{avg}$ , and $d_c$ as parameter $d_v$ increases. The parameter $\omega = 2$ was fixed	31
2.18	Werner state contour plots of SQT $F_{avg}$ as function of the coupling strenght $d_c$ . . . . .	33
2.19	Contour plot coupling $d_c$ parameter and environment $d_v$ , with noise $\sigma_z$ acting over one qubit. a) Bell's state, b),c),d) are Werner states. For all the plots the value $\omega = 2$ has been fixed. . . . .	35
2.20	The SQT $F_{avg}$ vs. coupling strength $d_c$ , with noise $\sigma_z$ acting over one qubit. The graph shows the behavior as environment parameter $d_v$ increase. $F_{avg}$ shows the Non-Markovian behavior just when environment parameter $d_v$ is large enough, for example in the last plots just c) and d) show to be in the Non-Markovian regime. For all the plots the parameter $\omega = 2$ was fixed. . . . .	36
2.21	The CQT fidelity, and non-controlled (NC) fidelity as a function of the coupling strength $d_c$ and environment parameter $d_c$ , where noise $\sigma_z$ is acting over one qubit. Parameter $\omega = 2$ has been fixed for the plots. . . . .	38
2.22	The CQT fidelity as a function of the coupling strenght $d_c$ . Environment parameter is fixed to a) $d_v = 6$ , and b) $d_v = 8$ . Parameter $\omega = 2$ is fixed for both plots. . . . .	39
2.23	Results obtained from inserting noise $\sigma_z$ in the first qubit of the quantum channel with the W state. Parameter $\omega = 2$ is fixed in all the plots . . . . .	40
2.24	Results obtained from inserting noise $\sigma_z$ in the second qubit of the quantum channel with the W state. Parameter $\omega = 2$ is fixed in all the plots. . . . .	41

# List of Tables

2.1 The different results for controlled fidelity, non-controlled fidelity and control power in terms of the different states for the CQT protocol . . . . . 37



# Chapter 1

## Introduction

### 1.1 Standard Quantum Teleportation

Quantum teleportation represents a process in which an unknown quantum state is transferred from the location A to the distant location B using both the classical and quantum channels, as shown in Fig.1. This transport of quantum information is reached without the physical transfer of the associated quantum information carrier [1]. Contrary to its classical approach, quantum teleportation is based on the use of quantum entanglement in order to perform the transfer of information tasks. The protocol mentioned above allows us to transmit this input quantum state using a relatively small amount of classical information; for example, the case of a two-level quantum system only requires two bits of classical information. The importance of this process lies in the ability to send any quantum information far huge distances, avoiding the exposure of our teleported states to decoherence from environments and other adverse effects.

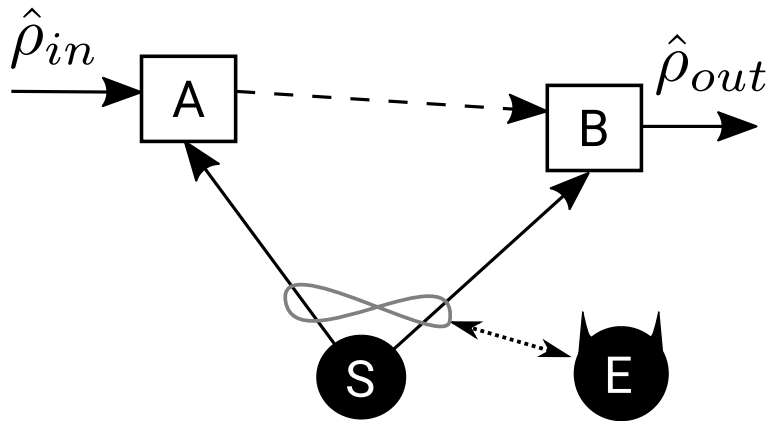


Figure 1.1: The basic scheme of quantum teleportation, where the letter A stands for the sending station and B for the receiving stations. The environment is marked as E. The solid lines represent quantum channels and dashed lines classical channels.

The first protocol to achieve quantum teleportation was first described by Bennet et al. [2], where they talk about how to teleport an unknown quantum state using a dual classical and Einstein-Podolsky-Rosen (EPR) channels. In order to board this protocol, we will define the positions A and B as the places where Alice and Bob stay, which are far away from each other. Then, the protocol is summarized as follows:

- i At first, an EPRs pair will be prepared and send to Alice and Bob, which corresponds to a quantum system with two qubits is created. The first qubit is sent to Alice, and the other one is sent to Bob. Such shared EPR state can be represented as:

$$|\Psi\rangle_{AB} = \frac{(|0\rangle_A \otimes |0\rangle_B + |1\rangle_A \otimes |1\rangle_B)}{\sqrt{2}} \quad (1.1)$$

where (1.1) is one of four maximally entangled two-qubit states, known as well as Bell states. This EPR pair now becomes our quantum channel.

- ii Then, Alice must perform a Bell measurement on one qubit of the EPR pair state  $|\Psi\rangle_A$ , and the input state  $|\Psi\rangle_{in}$  which she wants to transfer to Bob. This measurement provides four possible outcomes, reflecting one of the four possible Bell states.
- iii This measurement is encoded in two bits of classical information and send to Bob via a classical communication channel.
- iv Due to the measurement performed by Alice, the second qubit of  $|\Psi\rangle_{AB}$ , that Bob possesses, contains now the initial state  $|\Psi\rangle_{in}$ . However, Bob needs to apply the corrective unitary transformation (represented by the X and Z Pauli matrices) to be the protocol successful. Which operation he should apply is given by the two bits of classical information received from Alice.

Above described protocol has been experimentally realized, for the first time, in photonic systems [3]. If we want to illustrate this protocol, for example we should start by preparing an entangled channel, we could create a bell state described by:

$$|\psi^+\rangle = \frac{1}{\sqrt{2}}(|01\rangle + |10\rangle) \quad (1.2)$$

Since a half of the EPR must be sent to Alice and the other half to Bob, Alice will own two qubits. The first one is the target state to be teleported  $|\psi\rangle = \alpha|0\rangle + \beta|1\rangle$ , and the other corresponds to the first half of the EPR pair in equation 1.2. In the other hand Bob only owns his corresponding half of the EPR pair. Now the three qubit state is given by:

$$\begin{aligned} |\psi\rangle \otimes |\psi^+\rangle &= (\alpha|0\rangle + \beta|1\rangle) \otimes \frac{1}{\sqrt{2}}(|01\rangle + |10\rangle) \\ &= \frac{\alpha}{\sqrt{2}}(|001\rangle + |010\rangle) + \frac{\beta}{\sqrt{2}}(|101\rangle + |110\rangle). \end{aligned} \quad (1.3)$$

A measurement over the bell state is given by the states  $|\phi^+\rangle, |\phi^-\rangle, |\psi^+\rangle$ , and  $|\psi^-\rangle$  which conforms a Bell basis set. The above states can be used in order to expand the computational basis, obtaining:

$$\begin{aligned} |00\rangle &= \frac{1}{\sqrt{2}}(|\phi^+\rangle + |\phi^-\rangle), \\ |11\rangle &= \frac{1}{\sqrt{2}}(|\phi^+\rangle - |\phi^-\rangle), \\ |01\rangle &= \frac{1}{\sqrt{2}}(|\psi^+\rangle + |\psi^-\rangle), \\ |10\rangle &= \frac{1}{\sqrt{2}}(|\psi^+\rangle - |\psi^-\rangle). \end{aligned} \quad (1.4)$$

Once the above relations are inserted in equation 1.3 we arrive to the term:

$$\begin{aligned} |\psi\rangle \otimes |\psi^+\rangle &= \frac{\alpha}{2}(|\phi^+\rangle + |\phi^-\rangle)|1\rangle + \frac{\alpha}{2}(|\psi^+\rangle + |\psi^-\rangle)|0\rangle + \frac{\beta}{2}(|\psi^+\rangle - |\psi^-\rangle)|1\rangle + \frac{\beta}{2}(|\phi^+\rangle - |\phi^-\rangle)|0\rangle, \\ &= \frac{1}{2}|\psi^+\rangle(\alpha|0\rangle + \beta|1\rangle) + \frac{1}{2}|\psi^-\rangle(\alpha|0\rangle - \beta|1\rangle) + \frac{1}{2}|\phi^+\rangle(\alpha|1\rangle + \beta|0\rangle) + \frac{1}{2}|\phi^-\rangle(\alpha|1\rangle - \beta|0\rangle). \end{aligned} \quad (1.5)$$

Then Alice must perform the Bell measurement which will lead to obtain one of the four states  $|\phi^+\rangle, |\phi^-\rangle, |\psi^+\rangle$ , and  $|\psi^-\rangle$ , with equal probability equal to  $p = \frac{1}{4}$ . This Bell measurement can be expressed in standard measurement in the computational basis, using the unitary operation CNOT before the measurement. This operation will transform Bell states according to:

$$\begin{aligned} |\phi^+\rangle &\rightarrow |00\rangle, \\ |\phi^-\rangle &\rightarrow |11\rangle, \\ |\psi^+\rangle &\rightarrow |01\rangle, \\ |\psi^-\rangle &\rightarrow |10\rangle. \end{aligned} \tag{1.6}$$

Since Alice applies this unitary transformation just to her qubits, the global state becomes:

$$|\psi\rangle \otimes |\psi^+\rangle = \frac{1}{2}|01\rangle(\alpha|0\rangle + \beta|1\rangle) + \frac{1}{2}|10\rangle(\alpha|0\rangle - \beta|1\rangle) + \frac{1}{2}|00\rangle(\alpha|1\rangle + \beta|0\rangle) + \frac{1}{2}|11\rangle(\alpha|1\rangle - \beta|0\rangle). \tag{1.7}$$

Then Alice performs a measurement over her two qubits in the computational basis, obtaining one of the four possible outcomes 00, 01, 10, or 11. This measurement results in two bits of classical information which will be sent to Bob via a classical communication channel. This measurement also will cause the collapse of the Bob's particle leading to  $\alpha|0\rangle + \beta|1\rangle$ ,  $\alpha|0\rangle - \beta|1\rangle$ ,  $\alpha|1\rangle + \beta|0\rangle$ , and  $\alpha|1\rangle - \beta|0\rangle$ , depending on which classical bits 01, 10, 00, or 11 Alice measured respectively. Once Bob receives the two classical bits, he must perform a unitary operation depending on the information gathered through the classical communication channel in order to recover the target state  $|\psi\rangle$  sent by Alice.

## 1.2 Controlled Quantum Teleportation

In the previous section, we have introduced the standard quantum teleportation, which is based on the bipartite entangled states, but it has the potential to be extended to a multipartite one. The case of our interest is the tripartite variant of quantum teleportation, as proposed by Karlsson and Boureane [4], which is called the controlled quantum teleportation (CQT). In this case, we assume that our model will be similar to the previous one, with the main difference that for this one will appear the participation of a third party that will be called the controller. The role of the controller (or Charlie) is to guarantee the fidelity of teleportation to be in the quantum regime (higher than 2/3). As mentioned by Barasinski and Svozilik [5], the main resource to be this protocol effective is the localizable entanglement.

So from now, our system will consist of a set of three subsystems which are again separated far from each other. Alice at position A will still be the sender, and Bob at position B continues as the receiver. The only difference is now Charlie, at the point C, acting as a controller (see the Fig.2). Similarly to the previous case, for the standard quantum teleportation, the transference of information between particles will be carried out through both the classical and quantum channels. In this way, the CQT protocol can be described by the following steps:

- i The protocol is using an entangled state conformed by three qubits, where each one will be sent to Alice, Bob, and Charlie, respectively. A typical example is the Greenberger-Horne-Zeilinger (GHZ) state:

$$|\Psi\rangle_{ABC} = \frac{(|0\rangle_A \otimes |0\rangle_B \otimes |0\rangle_C + |1\rangle_A \otimes |1\rangle_B \otimes |1\rangle_C)}{\sqrt{2}} \tag{1.8}$$

- ii Once each of them has the corresponding qubit, Charlie will perform measurement over his qubit. The outcome measurement will be encoded in two bit of classical information and then shared with Bob only through classical channels if Charlie wants to allow the quantum teleportation.

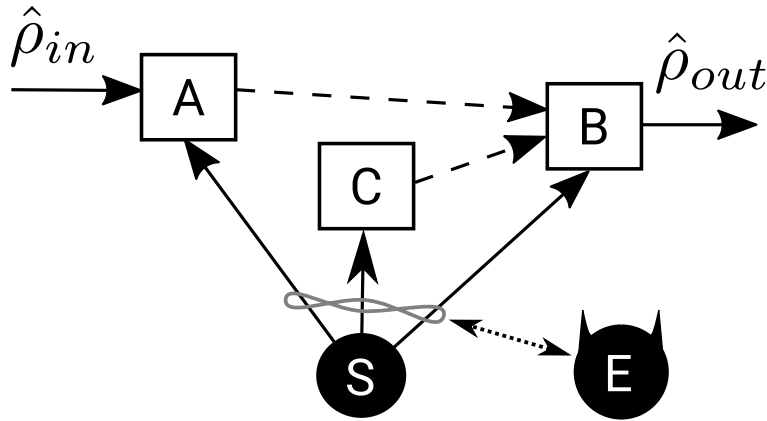


Figure 1.2: The scheme of the controlled quantum teleportation protocol. The letter A stands for the sending, B for receiving, and C for controller's stations. The environment is marked as E. The solid lines represent quantum channels and dashed lines classical channels.

- iii In a similar way, Alice will perform measurements over her EPR pair qubit and the qubit  $|\Psi\rangle_{in}$  she wishes to teleport to Bob. Her outcome measurement will be encoded in two bits and send to Bob.
- iv Now, depending on the information received from Alice and Charlie, Bob can modify his EPR pair in order to obtain a state identical to the input state  $|\Psi\rangle_{in}$ .

Just recently, the controlled quantum teleportation was experimentally presented in [6].

### 1.3 Quantum gates and quantum circuits

In order to describe the changes occurring to a quantum state in quantum computation we may use quantum gates. In classical computation a computer is built using logic gates, in the same way quantum computation can be done making use of the analogous operation known as quantum gates. This quantum gates are useful in order to manipulate the information. All the quantum gates can be expressed as unitary matrices, it means that a square complex matrix (representing a quantum gate) must be in accordance to  $UU^\dagger = U^\dagger U = I$ . In the case for a single qubit the main gates are:

$$\begin{aligned}
 X &= \begin{pmatrix} 0 & 1 \\ 1 & 0 \end{pmatrix} & Y &= \begin{pmatrix} 0 & -i \\ i & 0 \end{pmatrix} \\
 Z &= \begin{pmatrix} 1 & 0 \\ 0 & -1 \end{pmatrix} & H &= \frac{1}{\sqrt{2}} \begin{pmatrix} 1 & 1 \\ 1 & -1 \end{pmatrix}
 \end{aligned}$$

which acts over just on qubit, allowing us to manipulate this input qubit in order to apply the basic operations of quantum computing. X quantum gate is equivalent to NOT classical logic gate, Y and Z represent rotation of the qubit on the Bloch sphere, and Hadamard (H) gate creates a superposition of our single qubit. In a similar way this quantum gates can be applied onto multiple qubits which is the general case of the gates. Within this generalization we found a case known as controlled-Not gate, it has as input two qubits known as the control qubit and the target qubit respectively. In such case target qubit will flip or not depending on the control qubit following the rules:

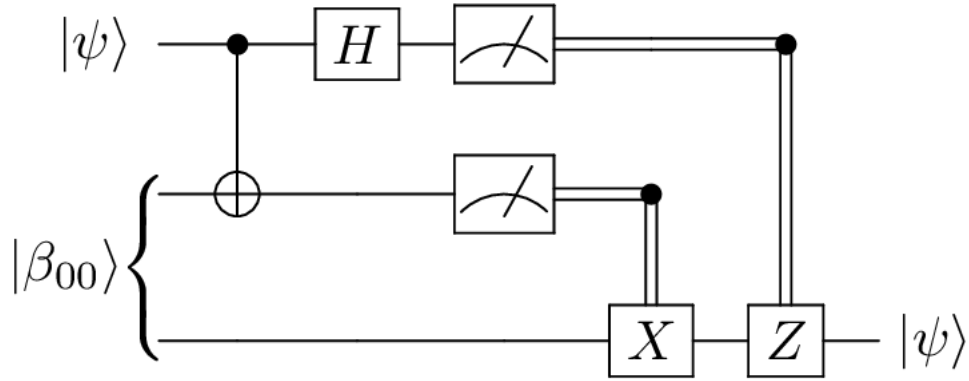


Figure 1.3: QT circuit conformed by the quantum gates CNOT, H, X, and Z. It is based in the Standard quantum teleportation protocol described above in the first section.

$|00\rangle \rightarrow |00\rangle, |01\rangle \rightarrow |01\rangle, |10\rangle \rightarrow |11\rangle, |11\rangle \rightarrow |10\rangle$ . This CNOT gate has a matrix representation given by:

$$CNOT = \begin{pmatrix} 1 & 0 & 0 & 0 \\ 0 & 1 & 0 & 0 \\ 0 & 0 & 0 & 1 \\ 0 & 0 & 1 & 0 \end{pmatrix} \quad (1.9)$$

These quantum gates can be put all together into a sequence in order to build quantum circuits. For example quantum teleportation protocol can be described through a quantum circuit as the one represented in figure 1.3.

Then the correspondent Unitary operation which describes the QT circuit can be described by the sequence of the employed quantum gates, operating them from right to the left as is represented by  $\hat{U}_{QT} = \hat{U}_{z13}\hat{U}_{c23}\hat{H}_1\hat{U}_{c12}$ , where the quantum gates are:

$$\hat{U}_{c12} = \begin{pmatrix} 1 & 0 & 0 & 0 & 0 & 0 & 0 & 0 \\ 0 & 1 & 0 & 0 & 0 & 0 & 0 & 0 \\ 0 & 0 & 1 & 0 & 0 & 0 & 0 & 0 \\ 0 & 0 & 0 & 1 & 0 & 0 & 0 & 0 \\ 0 & 0 & 0 & 0 & 0 & 0 & 1 & 0 \\ 0 & 0 & 0 & 0 & 0 & 0 & 0 & 1 \\ 0 & 0 & 0 & 0 & 1 & 0 & 0 & 0 \\ 0 & 0 & 0 & 0 & 0 & 1 & 0 & 0 \end{pmatrix} \quad \hat{H}_1 = \frac{1}{\sqrt{2}} \begin{pmatrix} 1 & 0 & 0 & 0 & 1 & 0 & 0 & 0 \\ 0 & 1 & 0 & 0 & 0 & 1 & 0 & 0 \\ 0 & 0 & 1 & 0 & 0 & 0 & 1 & 0 \\ 0 & 0 & 0 & 1 & 0 & 0 & 0 & 1 \\ 1 & 0 & 0 & 0 & -1 & 0 & 0 & 0 \\ 0 & 1 & 0 & 0 & 0 & -1 & 0 & 0 \\ 0 & 0 & 1 & 0 & 0 & 0 & -1 & 0 \\ 0 & 0 & 0 & 1 & 0 & 0 & 0 & -1 \end{pmatrix}$$

$$\hat{U}_{c23} = \begin{pmatrix} 1 & 0 & 0 & 0 & 0 & 0 & 0 & 0 \\ 0 & 1 & 0 & 0 & 0 & 0 & 0 & 0 \\ 0 & 0 & 0 & 1 & 0 & 0 & 0 & 0 \\ 0 & 0 & 1 & 0 & 0 & 0 & 0 & 0 \\ 0 & 0 & 0 & 0 & 1 & 0 & 0 & 0 \\ 0 & 0 & 0 & 0 & 0 & 1 & 0 & 0 \\ 0 & 0 & 0 & 0 & 0 & 0 & 1 & 0 \\ 0 & 0 & 0 & 0 & 0 & 0 & 1 & 0 \end{pmatrix} \quad \hat{U}_{z13} = \begin{pmatrix} 1 & 0 & 0 & 0 & 0 & 0 & 0 & 0 \\ 0 & 1 & 0 & 0 & 0 & 0 & 0 & 0 \\ 0 & 0 & 1 & 0 & 0 & 0 & 0 & 0 \\ 0 & 0 & 0 & 1 & 0 & 0 & 0 & 0 \\ 0 & 0 & 0 & 0 & 1 & 0 & 0 & 0 \\ 0 & 0 & 0 & 0 & 0 & -1 & 0 & 0 \\ 0 & 0 & 0 & 0 & 0 & 0 & 1 & 0 \\ 0 & 0 & 0 & 0 & 0 & 0 & 0 & -1 \end{pmatrix}$$

In the previous definitions for unitary operations sub-indices 1, 2, and 3 are used to point the different qubits in the



quantum circuit from the upper part to the lowest. In such case sub-indices 1, and 2 are the qubits owned by Alice, and 3 is the qubit owned by Bob. Qubits 2 and 3 are the corresponding qubits of the EPR pair. Finally the QT circuit can be expressed in its matrix form as:

$$\hat{U}_{QT} = \begin{pmatrix} \frac{1}{\sqrt{2}} & 0 & 0 & 0 & 0 & 0 & \frac{1}{\sqrt{2}} & 0 \\ 0 & \frac{1}{\sqrt{2}} & 0 & 0 & 0 & 0 & 0 & \frac{1}{\sqrt{2}} \\ 0 & 0 & 0 & \frac{1}{\sqrt{2}} & 0 & \frac{1}{\sqrt{2}} & 0 & 0 \\ 0 & 0 & \frac{1}{\sqrt{2}} & 0 & \frac{1}{\sqrt{2}} & 0 & 0 & 0 \\ \frac{1}{\sqrt{2}} & 0 & 0 & 0 & 0 & 0 & -\frac{1}{\sqrt{2}} & 0 \\ 0 & -\frac{1}{\sqrt{2}} & 0 & 0 & 0 & 0 & 0 & \frac{1}{\sqrt{2}} \\ 0 & 0 & 0 & \frac{1}{\sqrt{2}} & 0 & -\frac{1}{\sqrt{2}} & 0 & 0 \\ 0 & 0 & -\frac{1}{\sqrt{2}} & 0 & \frac{1}{\sqrt{2}} & 0 & 0 & 0 \end{pmatrix} \quad (1.10)$$

## 1.4 Fidelity as a quantitative description of protocol efficiency

In classical information protocols copying an unknown classical state is as easy as applying a CNOT operation over our state in order to get a copy of it. Since we are treating with quantum information, make an exact copy of an unknown state does not result such easy. According to the no-cloning theorem, it is impossible to make an exact copy of an unknown state [1]. In this sense, the use of EPR pairs is a helpful tool in order to apply the entanglement-assisted teleportation, in which in order to replicate an arbitrary unknown state, we destroy it in one place and further we reconstruct the exact state in another place. When we are using this principle to create a replica of these states, it is important to know with how large accuracy does our operation copy of the original state. In order to quantify this accuracy, the fidelity becomes a helpful tool which allows us to verify how good the quality of our copy is. This fidelity can be cataloged as a distance measure between two states, as this distance becomes closer to 1, we can be secure that both states are becoming more similar. The fidelity is a crucial tool in quantum communications since the transmission of information in the real world does not result as perfect as one could wish. For example, if we are trying to communicate a sequence of classical information, this transmission will decay in quality, since, according to Jozsa [7], it will be subject to:

- Limitations in the resources, requiring our data to be compressed before sending it
- The existence of random noise in the communication channels, which affects causing errors in data transmission.

In this way, such as in the classical regime, the quantum transmission of information can be affected, for example, by the quantum noise. Making use of this knowledge, we can extract information about the quality of our quantum teleportation process through the fidelity measurement. Fidelity measurement between two states is also known as the Uhlmann transition probability, and it is defined by the expression:

$$F(\rho, \sigma) = \left[ \text{Tr} \sqrt{\sqrt{\rho} \sigma \sqrt{\rho}} \right]^2, 0 \leq F \leq 1. \quad (1.11)$$

For example lets suppose we have the states  $|\psi\rangle = |1\rangle$ , and  $|\phi\rangle = |0\rangle$ . Then we can calculate their respective density operators as:

$$\rho = |1\rangle\langle 1| = \begin{pmatrix} 0 & 0 \\ 0 & 1 \end{pmatrix}, \quad (1.12)$$

$$\sigma = |0\rangle\langle 0| = \begin{pmatrix} 1 & 0 \\ 0 & 0 \end{pmatrix}. \quad (1.13)$$

Then the Fidelity between both states is given by:

$$\begin{aligned}
 F(\rho, \sigma) &= \left[ \text{Tr} \sqrt{\sqrt{\begin{pmatrix} 0 & 0 \\ 0 & 1 \end{pmatrix}} \begin{pmatrix} 1 & 0 \\ 0 & 0 \end{pmatrix} \sqrt{\begin{pmatrix} 0 & 0 \\ 0 & 1 \end{pmatrix}}} \right]^2 \\
 &= \left[ \text{Tr} \sqrt{\begin{pmatrix} 0 & 0 \\ 0 & 0 \end{pmatrix}} \right]^2 \\
 &= 0.
 \end{aligned} \tag{1.14}$$

Fidelity can be within the range  $[0, 1]$ , where the value of 1 stands for identical states, and 0 for the opposite states. From Jozsa [7], we can find some properties of the fidelity, such as it is symmetric, non-negative, continuous, a concave function of both states, unitarily invariant, equal to unity if and only if both states do coincide. Its properties made it a fantastic candidate in order to characterize the preservation of our states through quantum communication.

## 1.5 Transmission Through Noisy Channels

According with the last sections, when we are performing task which involves the transmission of information, we are assuming that there can exist some lost of the integrity of the information. The interaction of our system with the environment for example, can affect the coherence of a state. Loss of coherence may mean that our entangled state becomes a mixed state, causing the loss of fidelity in the teleportation process consequently. According to Nielsen Chuang [1], this interaction within our protocols can be present in different steps as: i) States to be teleported are mixed, ii) Quantum channels are noisy, and iii) Noise during the Bell Measurement and corrective unitary operation. In order to observe how this noise is affecting the accuracy of the teleportation process, a solution for the master equation is necessary. The Master equation consists of an expression that allows us to introduce and describe noise in continuous time for a given system. The most common form of this equation is given in the form of Lindblad equation which is [8]:

$$\frac{d\rho}{dt} = -\frac{i}{\hbar}[H, \rho] + \sum_{i,\alpha} \left( L_{i,\alpha} \rho L_{i,\alpha}^\dagger - \frac{1}{2} \{L_{i,\alpha}^\dagger L_{i,\alpha}, \rho\} \right) \tag{1.15}$$

This is the most general form of Markovian master equation. When the first part corresponds to the time-free evolution of the density state  $\rho$  and the second part corresponding to the sum of terms, is time dependent. The  $L_{i,\alpha}$  operators are known as Lindblad operator describes the decoherence of the evolving system. Lindblad operator is defined according to [8] as:

$$L_{i,\alpha} = \sqrt{\gamma_{i,\alpha}} \sigma_i^{(\alpha)}, \tag{1.16}$$

where the sub-index  $i$  indicates the qubit over which decoherence is acting, and  $\alpha$  sub-index stands for the type of decoherence introduced to system with  $\alpha = x, y, z$ . The X, Y, and Z are Pauli matrices and works introducing decoherence in a specific direction. The  $\gamma$  parameter is a eigenvalue from a diagonal positive semidefinite matrix. This  $\gamma$  parameter also allow us to control the noise switching it on and off.

## 1.6 Non-Markovian Dynamics

As introduced above, our system can not be thought of as an ideal one since it is an open systems that is subject to interactions with the environment. This unavoidable interaction generates a system-environment correlation, which

means a loss of coherence in our system [8]. In this sense, A non-Markovian system could be understood as the memory effects existing in an environment, such that they totally depend on the exchange of information between the system and the environment. If we think about this flow of information, we could basically have two scenarios: the first one in which the system is losing information constantly as it evolves in time (which is the Markovian case), and a second one in which system and environment interchange information in both flow directions, in this way the system is losing and recovery information from the environment (the non-Markovian case). According to Breuer et al.[8], "quantum non-Markovianity is associated with the notion of quantum memory". As mentioned previously, the use of fidelity results very useful in order to characterize how close are two states, then this idea can also be employed to express how memory effects are affecting in our case. If we continue thinking about the quantum teleportation, immediately comes to us, the idea of Alice preparing a state to be sent to Bob. If the prepared state is in a system which is coupled to the environment, as the system starts to lose information, then they are experimenting an effect that can be described as similar to sending some information through a noisy channel, which will produce a further loss of the fidelity between the state to be sent by Alice and the one that Bob is receiving. If these losses of fidelity are continuous in time, we may say that the system is experimenting the Markovian behavior. Conversely, if the behavior in time results nonmonotonic, it means that for a determined period of time, the fidelity starts to increase, then we are talking about the non-Markovian behavior. Since there exists a bidirectional flow of information, the system starts losing information that is stored by the environment and then given back to the system, influencing the system.

## Chapter 2

# Results & Discussion

### 2.1 Standard Quantum Teleportation

For the first part, we demonstrate how under a non-entangled channel, our fidelity is upper limited by the classical limit fidelity  $\frac{2}{3}$ . In this case, our non-entangled channel is given by:

$$|\psi_{non}\rangle = |0_A 0_B\rangle \quad (2.1)$$

With the input state described by:

$$|\psi_{in}\rangle = \cos\left(\frac{\theta}{2}\right)|0\rangle + e^{i\phi}\sin\left(\frac{\theta}{2}\right)|1\rangle \quad (2.2)$$

Which have the correspondent density operators:

$$\hat{\rho}_{AB} = \begin{pmatrix} 1 & 0 & 0 & 0 \\ 0 & 0 & 0 & 0 \\ 0 & 0 & 0 & 0 \\ 0 & 0 & 0 & 0 \end{pmatrix}, \quad (2.3)$$

$$\hat{\rho}_{in} = \begin{pmatrix} \cos^2\left(\frac{\theta}{2}\right) & e^{-i\phi}\sin\left(\frac{\theta}{2}\right)\cos\left(\frac{\theta}{2}\right) \\ e^{i\phi}\sin\left(\frac{\theta}{2}\right)\cos\left(\frac{\theta}{2}\right) & \sin^2\left(\frac{\theta}{2}\right) \end{pmatrix} \quad (2.4)$$

Then the full density operator for our system is given as:

$$\hat{\rho} = \hat{\rho}_{in} \otimes \hat{\rho}_{AB} = \begin{pmatrix} \cos^2\frac{\theta}{2} & 0 & 0 & 0 & e^{-i\phi}\cos\frac{\theta}{2}\sin\frac{\theta}{2} & 0 & 0 & 0 \\ 0 & 0 & 0 & 0 & 0 & 0 & 0 & 0 \\ 0 & 0 & 0 & 0 & 0 & 0 & 0 & 0 \\ 0 & 0 & 0 & 0 & 0 & 0 & 0 & 0 \\ e^{i\phi}\cos\frac{\theta}{2}\sin\frac{\theta}{2} & 0 & 0 & 0 & \sin^2\frac{\theta}{2} & 0 & 0 & 0 \\ 0 & 0 & 0 & 0 & 0 & 0 & 0 & 0 \\ 0 & 0 & 0 & 0 & 0 & 0 & 0 & 0 \\ 0 & 0 & 0 & 0 & 0 & 0 & 0 & 0 \end{pmatrix}, \quad (2.5)$$

where  $\hat{\rho}_{in} = |\psi_{in}\rangle\langle\psi_{in}|$  and  $\hat{\rho}_{AB} = |\psi_{non}\rangle\langle\psi_{non}|$ .

The output state is obtained as:

$$\begin{aligned} \hat{\rho}_{out} &= Tr_{AB} \left[ \hat{U}_{qt} (\hat{\rho}_{in} \otimes \hat{\rho}_{AB}) \hat{U}_{qt}^\dagger \right], \\ &= Tr_{AB} \begin{bmatrix} \frac{1}{2} \cos^2\left(\frac{\theta}{2}\right) & 0 & 0 & \frac{1}{4} e^{-i\phi} \sin(\theta) & \frac{1}{2} \cos^2\left(\frac{\theta}{2}\right) & 0 & 0 & \frac{1}{4} e^{-i\phi} \sin(\theta) \\ 0 & 0 & 0 & 0 & 0 & 0 & 0 & 0 \\ 0 & 0 & 0 & 0 & 0 & 0 & 0 & 0 \\ \frac{1}{4} e^{i\phi} \sin(\theta) & 0 & 0 & \frac{1}{2} \sin^2\left(\frac{\theta}{2}\right) & \frac{1}{4} e^{i\phi} \sin(\theta) & 0 & 0 & \frac{1}{2} \sin^2\left(\frac{\theta}{2}\right) \\ \frac{1}{2} \cos^2\left(\frac{\theta}{2}\right) & 0 & 0 & \frac{1}{4} e^{-i\phi} \sin(\theta) & \frac{1}{2} \cos^2\left(\frac{\theta}{2}\right) & 0 & 0 & \frac{1}{4} e^{-i\phi} \sin(\theta) \\ 0 & 0 & 0 & 0 & 0 & 0 & 0 & 0 \\ 0 & 0 & 0 & 0 & 0 & 0 & 0 & 0 \\ \frac{1}{4} e^{i\phi} \sin(\theta) & 0 & 0 & \frac{1}{2} \sin^2\left(\frac{\theta}{2}\right) & \frac{1}{4} e^{i\phi} \sin(\theta) & 0 & 0 & \frac{1}{2} \sin^2\left(\frac{\theta}{2}\right) \end{bmatrix} \end{aligned} \quad (2.6)$$

where the operator  $\hat{U}_{qt}$  describing the standard teleportation protocol is defined as:

$$\hat{U}_{qt} = \hat{U}_{z13} \hat{U}_{c23} \hat{H}_1 \hat{U}_{c12}. \quad (2.7)$$

Here, we use numbers 1-3 to distinguish different qubits, 1 corresponds to the input state, 2 and 3 to the quantum channel. The appearing operators are:  $\hat{H}$  is the Hadamard operator,  $\hat{U}_c$  is the C-NOT, and  $\hat{U}_z$  is the C-Z. [1]

With the output teleported state:

$$\hat{\rho}_{out} = \begin{pmatrix} \cos^2 \frac{\theta}{2} & 0 \\ 0 & \sin^2 \frac{\theta}{2} \end{pmatrix} \quad (2.8)$$

Which has the respective values for the fidelity and the average Fidelity:

$$\begin{aligned} F &= \langle \psi_{in} | \hat{\rho}_{out} | \psi_{in} \rangle, \\ &= \begin{pmatrix} \cos^2 \frac{\theta}{2} & e^{-i\phi} \sin \frac{\theta}{2} \end{pmatrix} \begin{pmatrix} \cos^2 \frac{\theta}{2} & 0 \\ 0 & \sin^2 \frac{\theta}{2} \end{pmatrix} \begin{pmatrix} \cos^2 \frac{\theta}{2} \\ e^{i\phi} \sin \frac{\theta}{2} \end{pmatrix}, \\ &= \frac{1}{4} (3 + \cos 2\theta) \end{aligned} \quad (2.9)$$

and with average fidelity calculated as:

$$\begin{aligned} F_{avg} &= \frac{1}{4\pi} \int_0^\pi d\theta \int_0^{2\pi} d\phi F(\theta, \psi) \sin(\theta), \\ &= \frac{1}{4\pi} \int_0^\pi d\theta \int_0^{2\pi} d\phi \frac{1}{4} (3 + \cos 2\theta) \sin(\theta), \\ &= \frac{1}{8} \int_0^\pi d\theta (3 \sin(\theta) + \cos 2\theta \sin(\theta)), \\ &= \frac{1}{8} (3 [-\cos \theta]_0^\pi + \frac{1}{2} ([-\cos \theta]_0^{3\pi} + [-\cos \theta]_0^\pi)) \\ &= \frac{2}{3} \end{aligned} \quad (2.10)$$

These values are consisted with the classical teleportation, since we are doing teleportation using a non-entangled classical channel. In this way for the classical teleportation protocol average fidelity is between 0, and  $\frac{2}{3}$ , which is also the upper limit for this case.

In the same way, proceeding as above, we can find the values given for our quantum teleportation protocol approach, in which we will use the entangled channel for our teleportation protocol. The entangled channel is:

$$\psi_{AB} = \frac{1}{\sqrt{2}}(|00\rangle + |11\rangle) \quad (2.11)$$

We will use the same input state given in 2.74, and the proceeding as in the previous case we will find that now the density matrix of the system is given by:

$$\hat{\rho} = \frac{1}{2} \begin{pmatrix} \cos^2 \frac{\theta}{2} & 0 & 0 & \cos^2 \frac{\theta}{2} & \frac{1}{2} e^{i\phi} \sin \theta & 0 & 0 & \frac{1}{2} e^{i\phi} \sin \theta \\ 0 & 0 & 0 & 0 & 0 & 0 & 0 & 0 \\ 0 & 0 & 0 & 0 & 0 & 0 & 0 & 0 \\ \cos^2 \frac{\theta}{2} & 0 & 0 & \cos^2 \frac{\theta}{2} & \frac{1}{2} e^{i\phi} \sin \theta & 0 & 0 & \frac{1}{2} e^{i\phi} \sin \theta \\ \frac{1}{2} e^{-i\phi} \sin \theta & 0 & 0 & \frac{1}{2} e^{-i\phi} \sin \theta & \sin^2 \frac{\theta}{2} & 0 & 0 & \sin^2 \frac{\theta}{2} \\ 0 & 0 & 0 & 0 & 0 & 0 & 0 & 0 \\ 0 & 0 & 0 & 0 & 0 & 0 & 0 & 0 \\ \frac{1}{2} e^{-i\phi} \sin \theta & 0 & 0 & \frac{1}{2} e^{-i\phi} \sin \theta & \sin^2 \frac{\theta}{2} & 0 & 0 & \sin^2 \frac{\theta}{2} \end{pmatrix} \quad (2.12)$$

Giving an output state such that:

$$\hat{\rho}_{out} = \begin{pmatrix} \cos^2 \frac{\theta}{2} & \frac{1}{2} e^{i\phi} \sin \theta \\ \frac{1}{2} e^{-i\phi} \sin \theta & \sin^2 \frac{\theta}{2} \end{pmatrix} \quad (2.13)$$

Resulting in the calculated fidelity measurements:

$$F = 1 \quad (2.14)$$

$$F_{avg} = 1 \quad (2.15)$$

In the case that we have an entangled quantum channel, our fidelity will reach the maximum fidelity 1, as showed in Figure 3. Then we can establish how the fidelity of our system is related to the degree of entanglement of the system. In order to achieve this goal we can characterize the behaviour for a generalized Bell state:

$$|\psi\rangle = p|00\rangle + \sqrt{1-p^2}|11\rangle, \quad (2.16)$$

where the parameter  $p$  belongs to the interval  $[0,1]$ .

Figure 2.1 shows the behavior of  $F_{AVG}$  depending on the parameter  $p$ . As we can observe, maximum fidelity is reached when  $p = \frac{1}{\sqrt{2}}$  which is consistant with the maximum quantum entangled Bell states. For the cases when  $p = 0$  and  $p = 1$ , when the state is separable,  $F_{avg}$  is in the classical limit, being consistent with what we showed previously. Since our system is not a closed one, it is subject to the interactions that the environment can generate over the system. This interaction leads to the existence of noise that will decrease the quality with which we will recover the initial state that is being teleported. As mentioned in the last section, we take into account such phenomena making use of equation 4. This master equation will allow us to observe the time evolution of our open system, and let us to include the effects of noise in our system communication channels.

## 2.1.1 Markovian Channel

### Fidelity Through Quantum Noise Channels

Since we are trying to learn about the behavior in time evolution we are going to use a variation of the established Lindblad equation 4, taking into account only those parts that will lead to an apparent change in the system, such that:

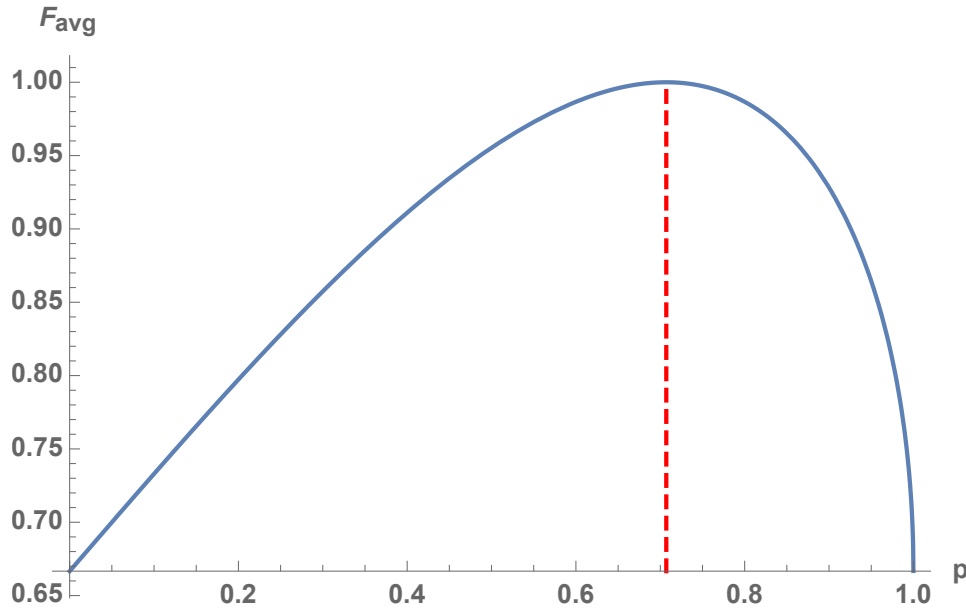


Figure 2.1: Measurements for the average fidelity vs. the parameter  $p$ . Red dashed line points the maximum of the function.

$$\frac{d\rho}{dt} = \sum_{i,\alpha} [L_{i,\alpha}\rho L_{i,\alpha}^\dagger - \frac{1}{2}\{L_{i,\alpha}^\dagger L_{i,\alpha}, \rho\}] \quad (2.17)$$

where the Lindblad operator  $L_{i,\alpha} = \sqrt{\gamma_{i,\alpha}}\sigma_i^{(\alpha)}$  describes the decoherence acting in direction  $i = x, y, z$  on the qubit ( $\alpha = 1, 2, 3$  or  $A, B, C$ ). From here we will define our initial density state as a matrix of  $t$  dependant variables similar to:

$$\rho(t)_{BC} = \rho(t)_{23} = \begin{pmatrix} C_{00}(t) & C_{01}(t) & C_{02}(t) & C_{03}(t) \\ C_{10}(t) & C_{11}(t) & C_{12}(t) & C_{13}(t) \\ C_{20}(t) & C_{21}(t) & C_{22}(t) & C_{23}(t) \\ C_{30}(t) & C_{31}(t) & C_{32}(t) & C_{33}(t) \end{pmatrix} \quad (2.18)$$

In this case we are going to model an entangled pair which is forming a quantum channel. We will study first the case where the quantum channel is subject to a noise which is only acting over the entangled qubit 2. Here some cases will be evaluated, using the Lindblad operators  $L_{2,z}$ ,  $L_{2,y}$ , and finally a mixture of both. In the second case, we will study our quantum channel subject to noise, but this time acting over both qubits, 2 and 3. This time we are going to evaluate three specific cases as will be described below. The introduction of the noise in entangled quantum channel will mean that our  $\rho_{ent}$  will be modified as described by  $\rho_{ent} \rightarrow \mathcal{E}(\rho_{ent})$ .

### Case 1: Noise over one channel in the Markovian regime

- (a) **Case 1a:** In this case we introduce a  $z$ -direction noise acting just in one of the entangled pair qubits. For this purpose we can define our Lindblad operator as  $L_{z,2} = \sqrt{\gamma_{z,2}}\sigma_z^{(2)}$ . Then the form of the Lindblad operator that will be used in the master equation given by  $L = L_{z,2} \otimes I_2$ . In a such way, our Lindblad equation is now

$\frac{d\rho}{dt} = L_{z,2}\rho L_{z,2}^\dagger - \frac{1}{2}\{L_{z,2}^\dagger L_{z,2}, \rho\}$  Then the differential equation given for our Master equation is:

$$\begin{pmatrix} \dot{C}_{00}(t) & \dot{C}_{01}(t) & \dot{C}_{02}(t) & \dot{C}_{03}(t) \\ \dot{C}_{10}(t) & \dot{C}_{11}(t) & \dot{C}_{12}(t) & \dot{C}_{13}(t) \\ \dot{C}_{20}(t) & \dot{C}_{21}(t) & \dot{C}_{22}(t) & \dot{C}_{23}(t) \\ \dot{C}_{30}(t) & \dot{C}_{31}(t) & \dot{C}_{32}(t) & \dot{C}_{33}(t) \end{pmatrix} = -2\gamma \begin{pmatrix} 0 & 0 & C_{02}(t) & C_{03}(t) \\ 0 & 0 & C_{12}(t) & C_{13}(t) \\ C_{20}(t) & C_{21}(t) & 0 & 0 \\ C_{30}(t) & C_{31}(t) & 0 & 0 \end{pmatrix} \quad (2.19)$$

leading us to the time evolved entangled density operator:

$$\varepsilon(\rho_{ent}(t)) = \begin{pmatrix} C_{00}(t) & C_{01}(t) & e^{-2\gamma t} C_{02}(t) & e^{-2\gamma t} C_{03}(t) \\ C_{10}(t) & C_{11}(t) & e^{-2\gamma t} C_{12}(t) & e^{-2\gamma t} C_{13}(t) \\ e^{-2\gamma t} C_{20}(t) & e^{-2\gamma t} C_{21}(t) & C_{22}(t) & C_{23}(t) \\ e^{-2\gamma t} C_{30}(t) & e^{-2\gamma t} C_{31}(t) & C_{32}(t) & C_{33}(t) \end{pmatrix} \quad (2.20)$$

From this point, it is possible to distinguish two paths to follow; the first one is when we use as our initial state density matrix, a fully entangled bell state which is:  $\rho_{ent}(0) = |\Phi^+\rangle\langle\Phi^+|$ , where  $|\Phi^+\rangle = \frac{1}{\sqrt{2}}(|00\rangle + |11\rangle)$ .

If we use that initial state in order to solve the unknowns  $C_{mn}$  in equation 2.20, they will become:  $C_{00}(t) = C_{03}(t) = C_{30}(t) = C_{33}(t) = \frac{1}{2}$  and all the remaining values correspond to zero. From this answer we can now obtain the output density matrix using  $\rho_{out} = Tr_{1,2}\{\hat{U}_{tel}\rho_{in} \otimes \varepsilon(\rho_{ent})\hat{U}_{tel}^\dagger\}$ . Then the output density matrix is:

$$\rho_{out} = \begin{pmatrix} \cos^2 \frac{\theta}{2} & \frac{1}{2} e^{-2\gamma t + i\phi} \sin \theta \\ \frac{1}{2} e^{-2\gamma t - i\phi} \sin \theta & \sin^2 \frac{\theta}{2} \end{pmatrix} \quad (2.21)$$

This expression now can be used to obtain the correspondent values for the fidelity and the average fidelity which are:

$$F(\theta, \phi) = \frac{1}{4}(3 + \cos 2\theta + 2e^{-2\gamma t} \sin^2 \theta) \quad (2.22)$$

$$F_{avg} = \frac{1}{3}(2 + e^{-2\gamma t}) \quad (2.23)$$

On the other hand we have the second path in which we are going to use the Werner state in order to study the teleportation performance for the initially partially mixed state with our initial density matrix, generating:  $\rho(0) = p|\Phi^+\rangle\langle\Phi^+| + (1-p)\frac{I_4}{4}$ . In this case, if we solve the unknowns in our evolved matrix 2.20, the resulting evolved density matrix will be:

$$\rho_{ent}(t) = \begin{pmatrix} \frac{p+1}{4} & 0 & 0 & \frac{1}{2} e^{-2\gamma t} p \\ 0 & \frac{1-p}{4} & 0 & 0 \\ 0 & 0 & \frac{1-p}{4} & 0 \\ \frac{1}{2} e^{-2\gamma t} p & 0 & 0 & \frac{p+1}{4} \end{pmatrix} \quad (2.24)$$

In standard quantum teleportation (SQT) protocol result in:

$$\rho_{out}(t) = \begin{pmatrix} \frac{1}{2}(p \cos(\theta) + 1) & \frac{1}{2} e^{-2\gamma t - i\phi} p \sin(\theta) \\ \frac{1}{2} e^{i\phi - 2\gamma t} p \sin(\theta) & \frac{1}{2}(1 - p \cos(\theta)) \end{pmatrix} \quad (2.25)$$

$$F = \frac{1}{4} e^{-2\gamma t} (p \cos(2\theta) (e^{2\gamma t} - 1) + (p+2)e^{2\gamma t} + p) \quad (2.26)$$

$$F_{avg} = \frac{1}{6} (2pe^{-2\gamma t} + p + 3) \quad (2.27)$$

All results are summarized in the Figures 2.2-2.4.



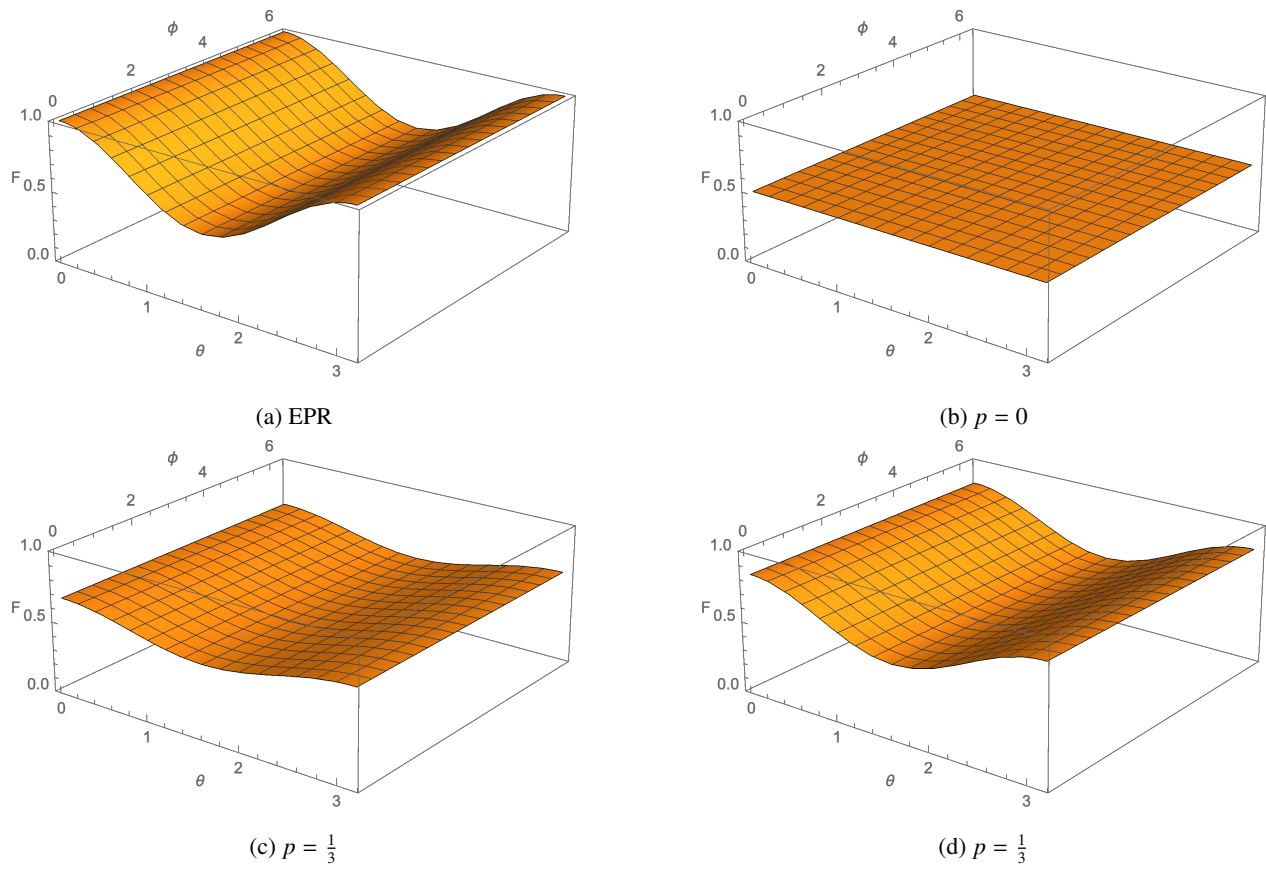


Figure 2.2: The SQT Fidelity vs  $\theta$  and  $\phi$  with the noise  $\sigma_z$  introduced in the second qubit. a) Bell's state, b), c), d) Werner states. For all the plots, the values  $t = 3$ ,  $\gamma = 1$  were fixed.

In figure 2.2 we can observe the Markovian dynamics of a system going under the effect of some decoherence introduced as noise acting over the z-direction. The maximum Fidelity will depend on the level of entanglement of the entangled channel, in the case of the EPR pair, Fidelity reaches its maximum value of 1. For the Werner states a similar behavior, but with the value for Fidelity decreasing as entanglement decreases.

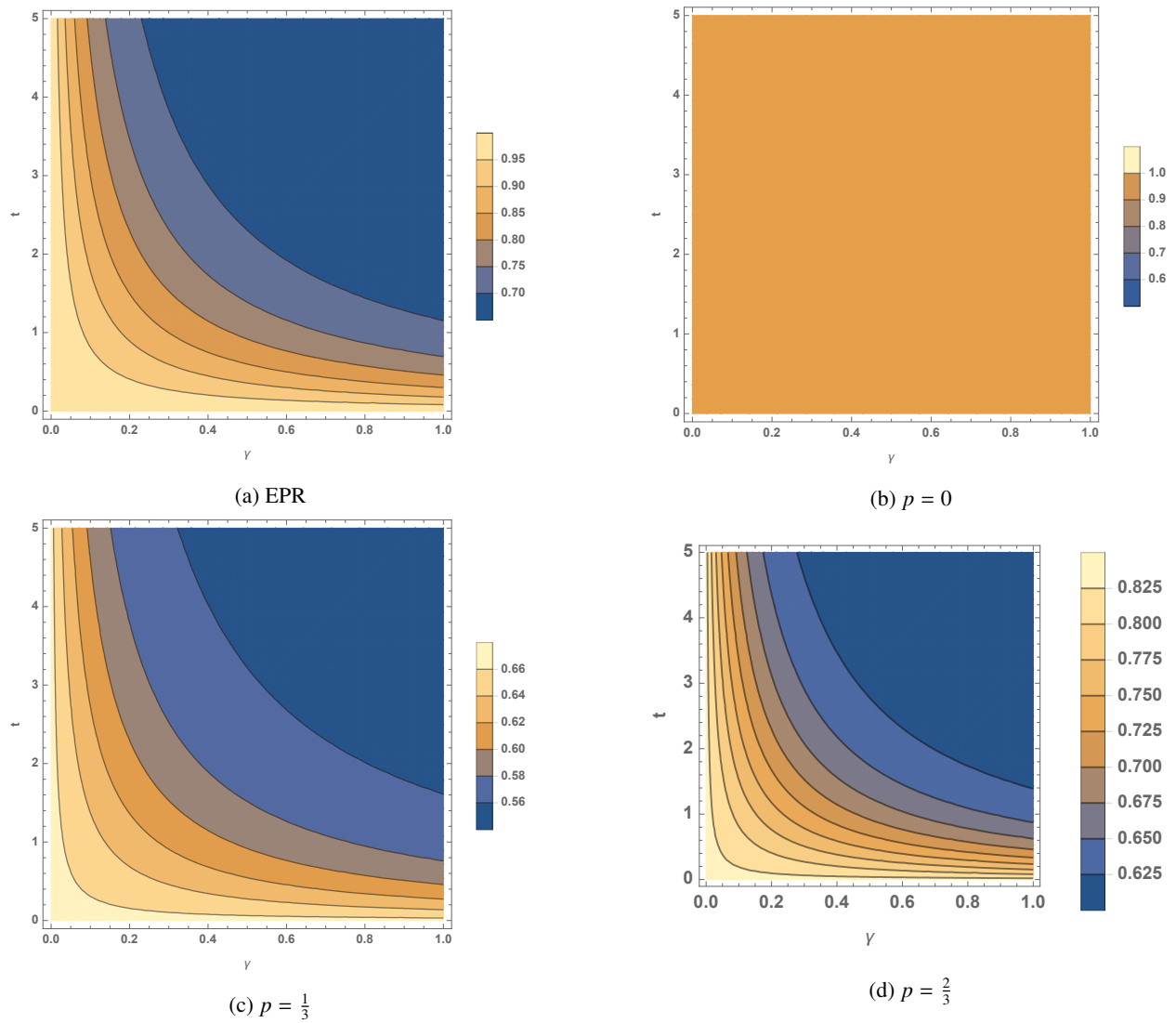


Figure 2.3: Contour plot of  $\gamma$  and  $t$  with the noise  $\sigma_z$  in the second qubit. Legends in the graphs show the behavior of  $F_{avg}$ . a) Bell's state, b), c), d) Werner states.

Figure 2.3 shows how is the behavior of the average fidelity of a system going under the effects of Markovian dynamics. Most of the graphs presents a more or less similar behavior, with the main difference in the maximum value for average fidelity. In the case of Werner state where entanglement is null, average fidelity shows a constant behavior and reaches the minimum value of all of the cases.

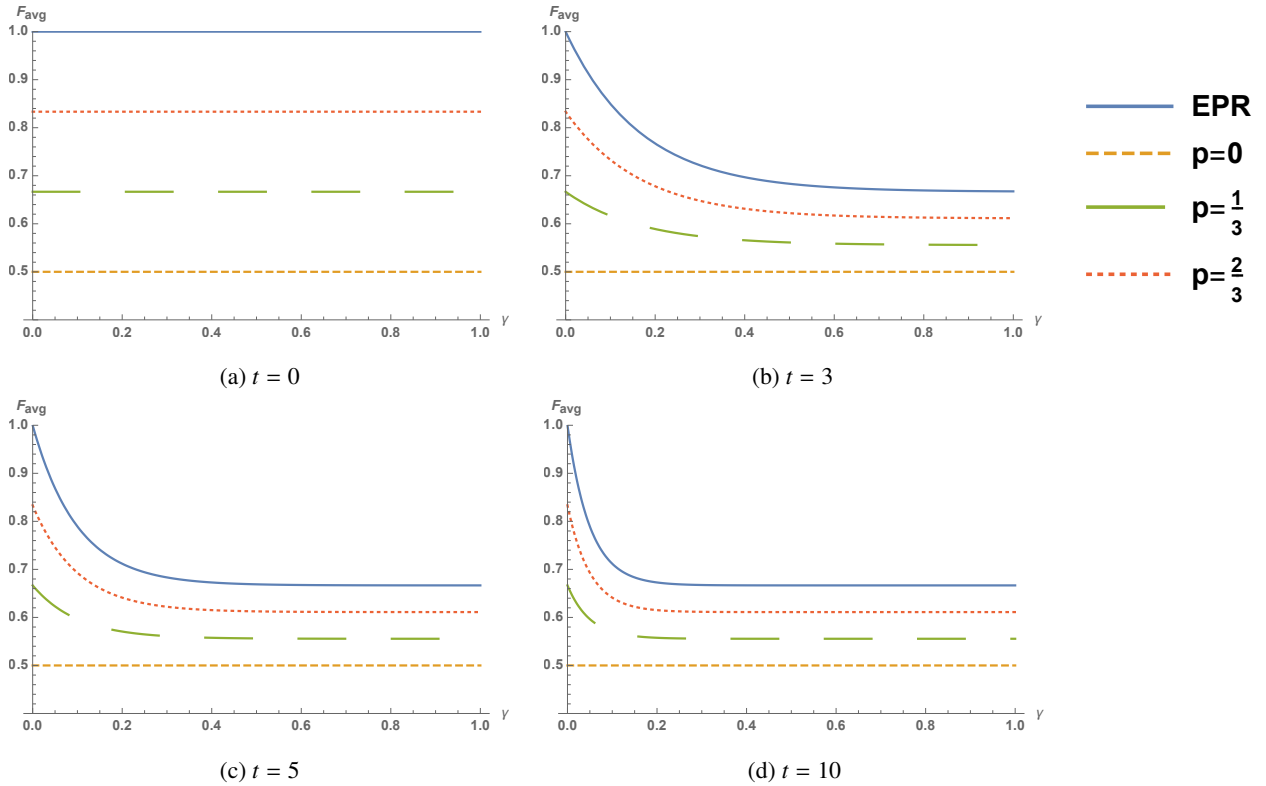


Figure 2.4: The SQT evolution of  $F_{avg}$  vs  $\gamma$ . Parameter  $t$  is fixed with values for a)  $t=0$ , b)  $t=3$ , c)  $t=5$ , d)  $t=10$

Figure 2.4 shows the behavior of Markovian Dynamics of the system through time. Again we observe how average fidelity decreases as entanglement becomes minimum. We also can observe how average fidelity decreases faster as  $\gamma$ , and  $t$  parameters become bigger.

- (b) **Case 1b:** For this case Lindblad operator  $L_{x,2} = \sqrt{\gamma_{x,2}}\sigma_x^{(2)}$  was employed. As in previous case decoherence is applied just in second qubit, but this time noise appears in the  $y$ -direction. The correspondent Lindblad equation for the system is:  $\frac{d\rho}{dt} = L_{x,2}\rho L_{x,2}^\dagger - \frac{1}{2}\{L_{x,2}^\dagger L_{x,2}, \rho\}$ , with the corresponding time evolved fully entangled density matrix:

$$\mathcal{E}(\rho_{ent}(t)) = \frac{1}{4}e^{-2t\gamma} \begin{pmatrix} 1 + e^{2t\gamma} & 0 & 0 & 1 + e^{2t\gamma} \\ 0 & -1 + e^{2t\gamma} & -1 + e^{2t\gamma} & 0 \\ 0 & -1 + e^{2t\gamma} & -1 + e^{2t\gamma} & 0 \\ 1 + e^{2t\gamma} & 0 & 0 & 1 + e^{2t\gamma} \end{pmatrix} \quad (2.28)$$

Once it is computed through the teleportation circuit, the output density matrix is given by:

$$\rho_{out} = \begin{pmatrix} \frac{1}{2}(e^{-2t\gamma} \cos(\theta) + 1) & \frac{1}{2} \sin(\theta) (\cos(\phi) - ie^{-2t\gamma} \sin(\phi)) \\ \frac{1}{2} \sin(\theta) (\cos(\phi) + e^{-2t\gamma} i \sin(\phi)) & \frac{1}{2} (1 - e^{-2t\gamma} \cos(\theta)) \end{pmatrix} \quad (2.29)$$

Which will result in the calculated fidelity functions as:

$$F = \frac{1}{16}e^{-2\gamma t - 2i\phi} \left( (1 + e^{2i\phi})^2 \cos(2\theta) (-e^{2\gamma t} - 1) + e^{4i\phi} (e^{2\gamma t} - 1) + 2e^{2i\phi} (5e^{2\gamma t} + 3) + e^{2\gamma t} - 1 \right) \quad (2.30)$$

$$F_{avg} = \frac{1}{3} (e^{-2\gamma t} + 2). \quad (2.31)$$

In the same way as in case 1a, we can also solve lindblad equation using the Werner state as the initial state. In that case our evolved density matrix will become:

$$\mathcal{E}(\rho_{ent}(t)) = \frac{1}{4} \begin{pmatrix} e^{-2\gamma t} p + 1 & 0 & 0 & (1 + e^{-2\gamma t}) p \\ 0 & 1 - e^{-2\gamma t} p & (1 - e^{-2\gamma t}) p & 0 \\ 0 & (1 - e^{-2\gamma t}) p & 1 - e^{-2\gamma t} p & 0 \\ (1 + e^{-2\gamma t}) p & 0 & 0 & e^{-2\gamma t} p + 1 \end{pmatrix} \quad (2.32)$$

Once it is applied in the SQT protocol, results are:

$$\rho_{out} = \frac{1}{2} \begin{pmatrix} (e^{-2\gamma t} p \cos(\theta) + 1) & p \sin(\theta) (\cos(\phi) - i e^{-2\gamma t} \sin(\phi)) \\ p \sin(\theta) (\cos(\phi) + e^{-2\gamma t} i \sin(\phi)) & (1 - e^{-2\gamma t} p \cos(\theta)) \end{pmatrix} \quad (2.33)$$

$$F = \frac{1}{8} e^{-2\gamma t - 2i\phi} (p (e^{2\gamma t} - 1)) ((1 + e^{4i\phi}) \sin^2(\theta) - e^{2i\phi} \cos(2\theta)) + e^{2i\phi} ((p + 4)e^{2\gamma t} + 3p), \quad (2.34)$$

$$F_{avg} = \frac{1}{6} (2p e^{-2\gamma t} + p + 3). \quad (2.35)$$

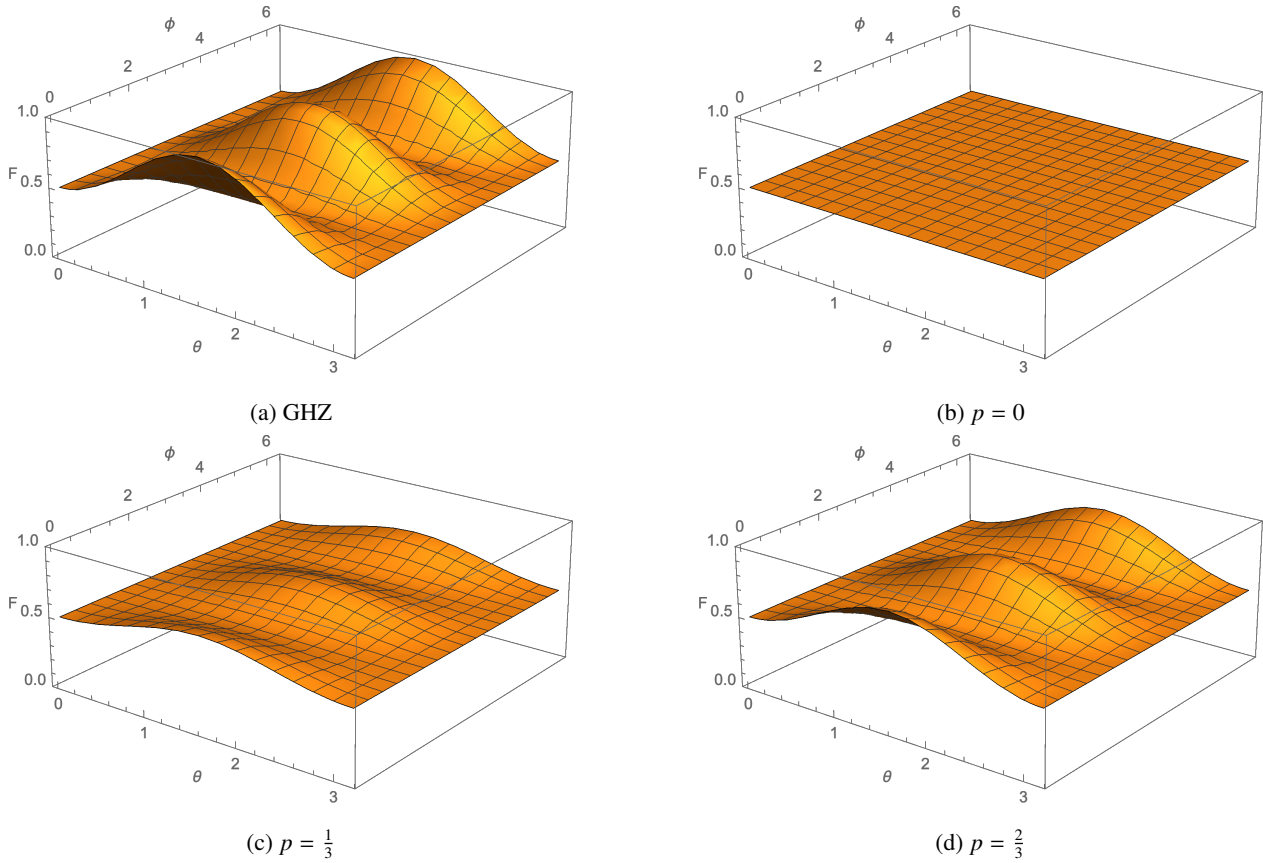


Figure 2.5: The SQT Fidelity vs  $\theta$  and  $\phi$  with the noise  $\sigma_x$  introduced in the second qubit. a) Bell's state, b), c), d) Werner states.

In figure 2.5 we observe the behavior of fidelity in a system under the effects of decoherence introduced as noise acting in the x-direction. Maximum fidelity will depend on both the angles of  $\phi$  and  $\theta$ , and the entanglement of the quantum channel.

**Case 1c:** In this part noise is going to be inserted in the system using  $L_{y,2} = \sqrt{\gamma_{y,2}}\sigma_y^{(2)}$ . Again the noise is only acting over just one channel, and it is propagating in y-direction. Then it can be introduced in our Lindblad equation in order to get the expression:  $\frac{d\rho}{dt} = L_{y,2}\rho L_{y,2}^\dagger - \frac{1}{2}\{L_{y,2}^\dagger L_{y,2}, \rho\}$ . When we evaluate our answer using the bell states, it gives us as result the evolved density matrix for the entangled channel:

$$\mathcal{E}(\rho_{ent}(t)) = \frac{1}{4}e^{-2\gamma t} \begin{pmatrix} 1 + e^{2\gamma t} & 0 & 0 & 1 + e^{2\gamma t} \\ 0 & -1 + e^{2\gamma t} & 1 - e^{2\gamma t} & 0 \\ 0 & 1 - e^{2\gamma t} & -1 + e^{2\gamma t} & 0 \\ 1 + e^{2\gamma t} & 0 & 0 & 1 + e^{2\gamma t} \end{pmatrix} \quad (2.36)$$

When (2.36) is used in the SQT protocol we obtain as result:

$$F = \frac{1}{8}e^{-2\gamma t - 2i\phi} \left( (1 + e^{4i\phi}) \sin^2(\theta) (-e^{2\gamma t} - 1) - e^{2i\phi} \cos(2\theta) (e^{2\gamma t} - 1) + e^{2i\phi} (5e^{2\gamma t} + 3) \right), \quad (2.37)$$

$$F_{avg} = \frac{1}{3} (e^{-2\gamma t} + 2). \quad (2.38)$$

It also can be computed for the case where the initial state is a Werner state, then our evolved density matrix becomes:

$$\mathcal{E}(\rho_{ent}(t)) = \frac{1}{4} \begin{pmatrix} e^{-2\gamma t} p + 1 & 0 & 0 & (1 + e^{-2\gamma t}) p \\ 0 & 1 - e^{-2\gamma t} p & (-1 + e^{-2\gamma t}) p & 0 \\ 0 & (-1 + e^{-2\gamma t}) p & 1 - e^{-2\gamma t} p & 0 \\ (1 + e^{-2\gamma t}) p & 0 & 0 & e^{-2\gamma t} p + 1 \end{pmatrix} \quad (2.39)$$

When it is transformed by the SQT circuit, then our results are:

$$F = \frac{1}{8}e^{-2\gamma t - 2i\phi} \left( e^{2i\phi} ((p + 4)e^{2\gamma t} + 3p) - p(e^{2\gamma t} - 1) ((1 + e^{4i\phi}) \sin^2(\theta) + e^{2i\phi} \cos(2\theta)) \right), \quad (2.40)$$

$$F_{avg} = \frac{1}{6} (2pe^{-2\gamma t} + p + 3) \quad (2.41)$$

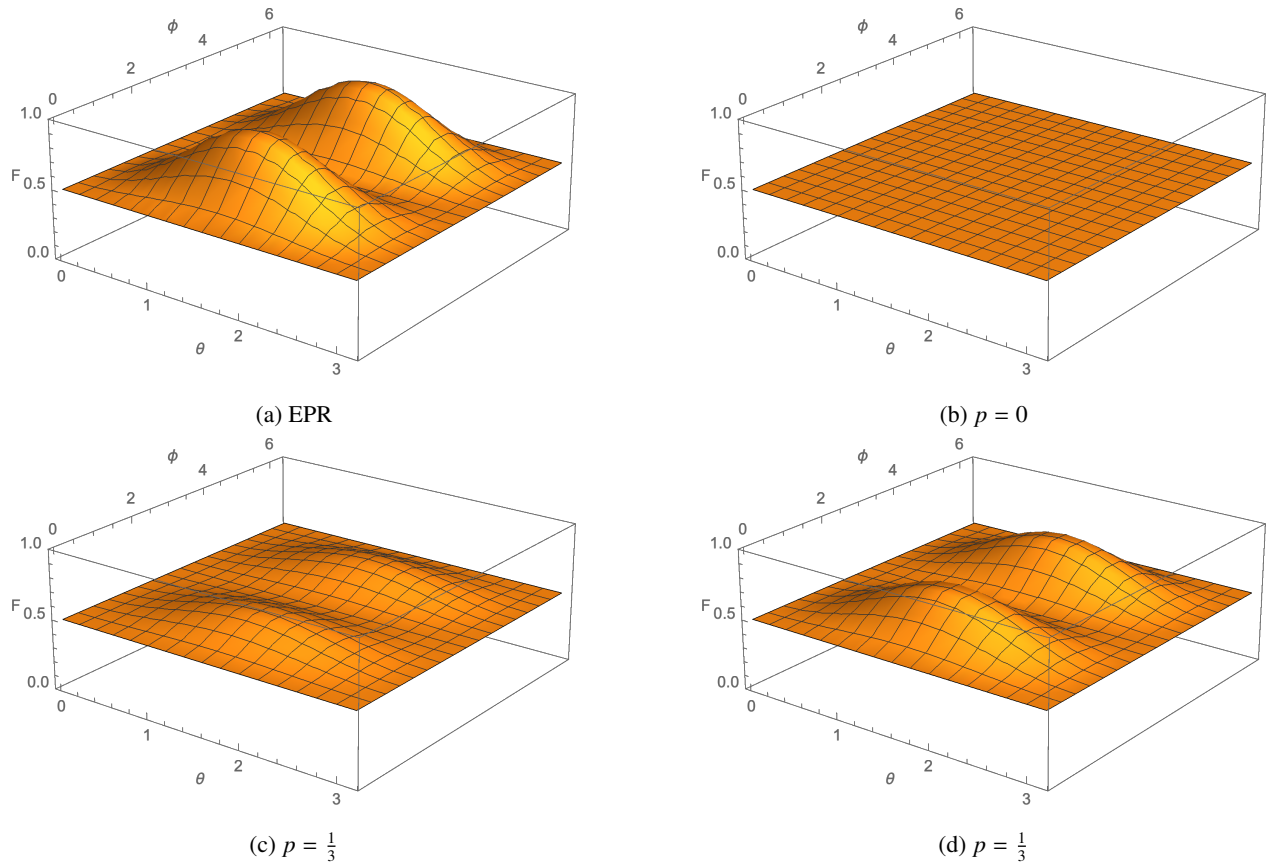


Figure 2.6: The SQT Fidelity vs  $\theta$  and  $\phi$  with the noise  $\sigma_y$  introduced in the second qubit. a) Bell's state, b), c), d) Werner states.

Similar to previous cases, in figure 2.6 we observe the dependence of fidelity in a system under Markovian dynamic, but this time with noise acting over y-direction. Like in the previous cases Fidelity depends on the angles  $\theta$ , and  $\phi$ , and the level of entanglement.

### Case 2: Noise over two channels in the Markovian regime

- (a) **Case 2a:** Contrary to the case 1, for this case noise in both qubits of the entangled pair quantum channel is introduced. Proceeding as previously we can define our Lindblad operators as:  $L_{z,2} = \sqrt{\gamma_{z,2}}\sigma_z^{(2)}$ , and  $L_{z,3} = \sqrt{\gamma_{z,3}}\sigma_z^{(3)}$ , with  $\gamma_{z,2} = \gamma_{z,3}$ . As we can notice in the previous expressions system still subject to noise just in z-direction. The Lindblad equation for this case is of the form:  $\frac{d\rho}{dt} = L_{z,2}\rho L_{z,2}^\dagger - \frac{1}{2}\{L_{z,2}^\dagger L_{z,2}, \rho\} + L_{z,3}\rho L_{z,3}^\dagger - \frac{1}{2}\{L_{z,3}^\dagger L_{z,3}, \rho\}$ . Then replacing in the master equation it will appear:

$$\begin{pmatrix} \dot{C}_{00}(t) & \dot{C}_{01}(t) & \dot{C}_{02}(t) & \dot{C}_{03}(t) \\ \dot{C}_{10}(t) & \dot{C}_{11}(t) & \dot{C}_{12}(t) & \dot{C}_{13}(t) \\ \dot{C}_{20}(t) & \dot{C}_{21}(t) & \dot{C}_{22}(t) & \dot{C}_{23}(t) \\ \dot{C}_{30}(t) & \dot{C}_{31}(t) & \dot{C}_{32}(t) & \dot{C}_{33}(t) \end{pmatrix} = -2\gamma \begin{pmatrix} 0 & C_{01}(t) & C_{02}(t) & 2C_{03}(t) \\ C_{10}(t) & 0 & 2C_{12}(t) & C_{13}(t) \\ C_{20}(t) & 2C_{21}(t) & 0 & C_{23}(t) \\ 2C_{30}(t) & C_{31}(t) & C_{32}(t) & 0 \end{pmatrix} \quad (2.42)$$

And using the same initial condition as in the case 1, our time evolved density matrix is equal to:

$$\varepsilon(\rho_{em}(t)) = \begin{pmatrix} 0 & -2\gamma C_{01}(t) & -2\gamma C_{02}(t) & -4\gamma C_{03}(t) \\ -2\gamma C_{10}(t) & 0 & -4\gamma C_{12}(t) & -2\gamma C_{13}(t) \\ -2\gamma C_{20}(t) & -4\gamma C_{21}(t) & 0 & -2\gamma C_{23}(t) \\ -4\gamma C_{30}(t) & -2\gamma C_{31}(t) & -2\gamma C_{32}(t) & 0 \end{pmatrix} \quad (2.43)$$

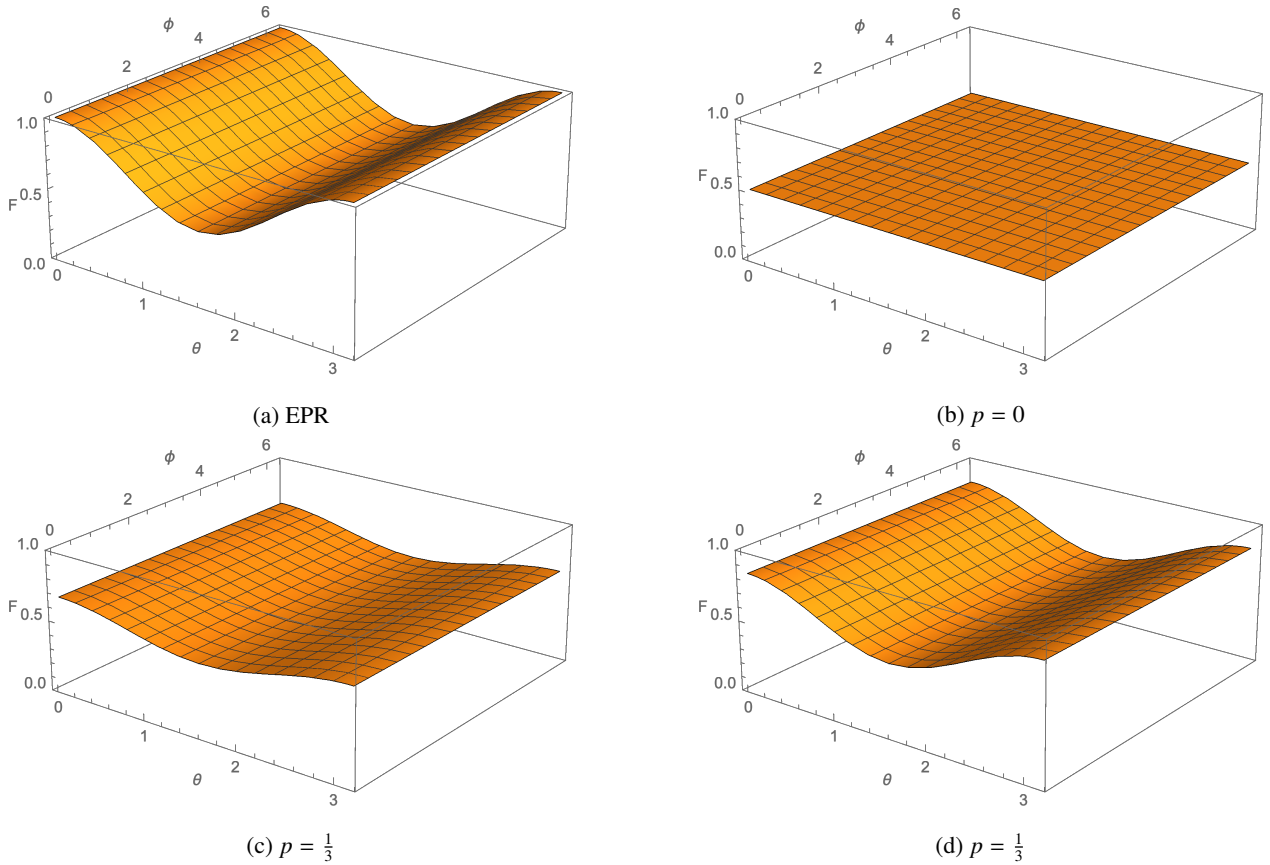


Figure 2.7: The SQT Fidelity vs  $\theta$  and  $\phi$  with the noise  $\sigma_z$  introduced in the first and second qubit. a) Bell's state, b), c), d) Werner states. Parameter  $t = 3$ , and  $\gamma = 1$  were fixed for all the plots

Despite of the existence of noise acting in two channels instead of just in one, in figure 2.10 we can observe a very similar behavior to the case of figure which noise  $i$ -z-direction acts over just one of the qubits.

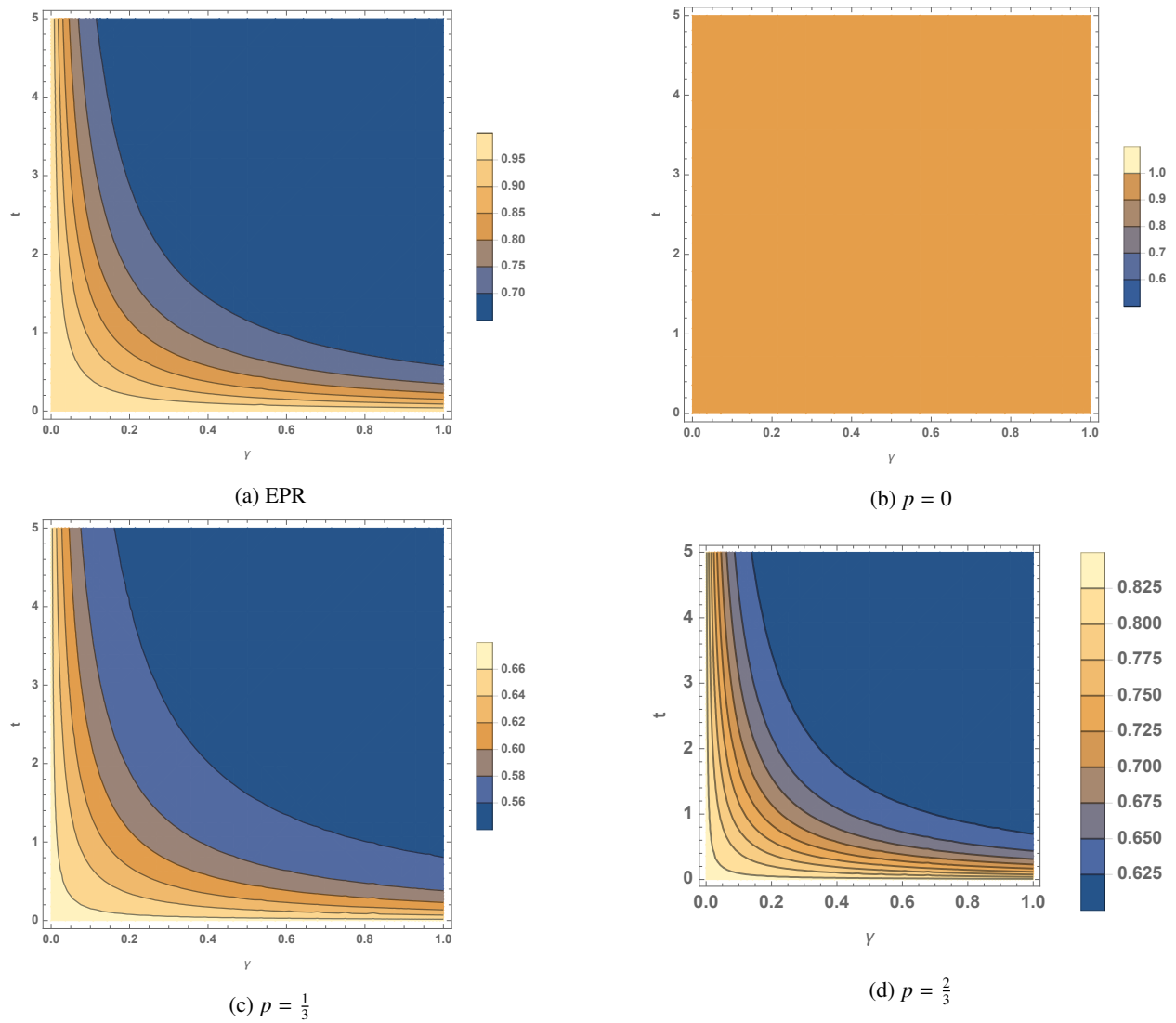


Figure 2.8: SQT Contour plot of  $\gamma$  and  $t$  with noise  $\sigma_z$  over both qubits. Legends in graphs show the  $F_{avg}$ . a) Bell's state, b), c), d) Werner states.

In figure 2.8 we observe a similar behavior with it analogous of the figure 2.3, but with the difference that average fidelity seems to decrease faster than the analogous case. This acceleration in decreasing of average fidelity could be caused by effects of noise inducing decoherence in the same direction over the two qubits.



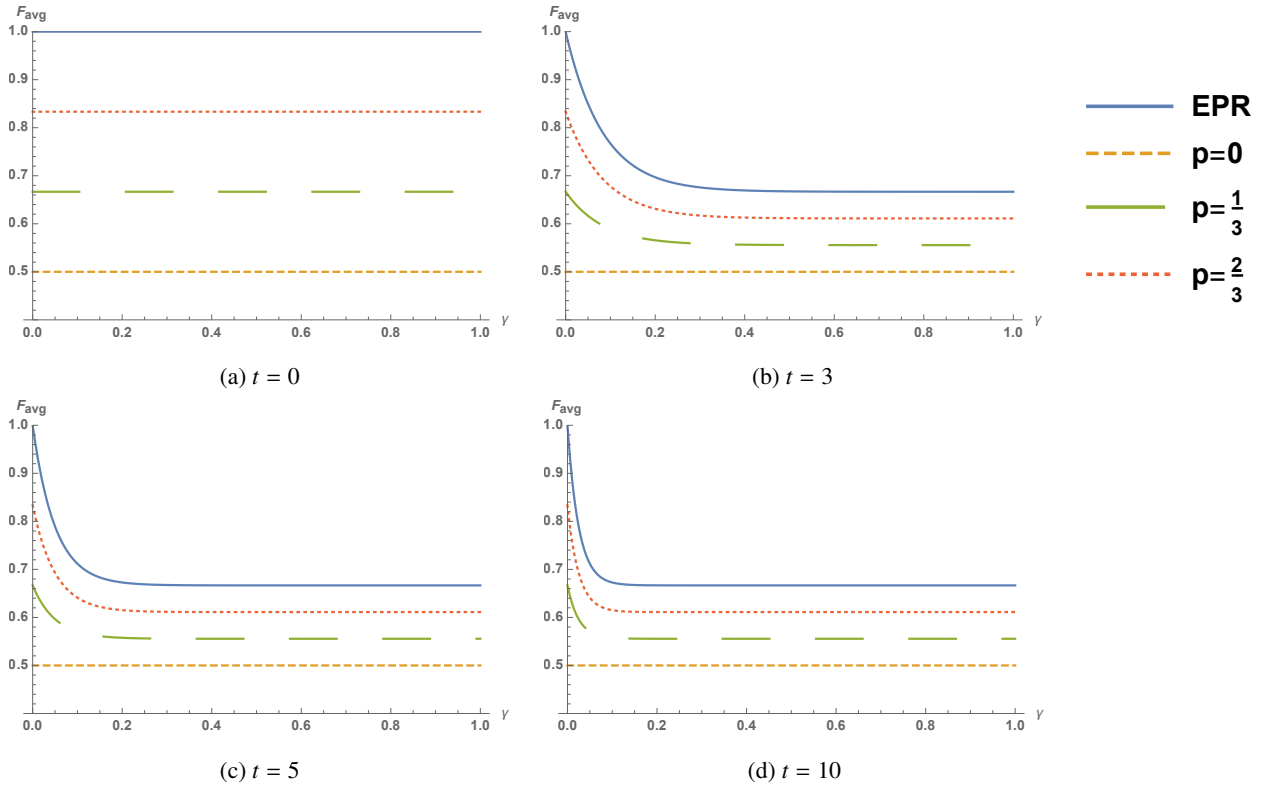


Figure 2.9: The SQT  $F_{avg}$  and  $\gamma$  through time with noise  $\sigma_z$  acting over both qubits. For the different plots the value for  $t$  was fixed as: a)  $t=0$ , b)  $t=3$ , c)  $t=5$ , d)  $t=10$

As  $t$  and  $\gamma$  parameter increases, average fidelity decreases faster. Comparing with its analogous case but with noise acting in only one qubit it also seem to lose coherence faster.

- (b) **Case 2b:** This case uses noise in the x-direction for both the equibit 2, and qubit 3, with Lindblad operators:  $L_{x,2} = \sqrt{\gamma_{x,2}}\sigma_z^{(2)}$ , and  $L_{x,3} = \sqrt{\gamma_{x,3}}\sigma_x^{(3)}$ , where  $\gamma_{x,2} = \gamma_{x,3}$ . From the previous part we know that our Lindblad equation is:  $\frac{d\rho}{dt} = L_{x,2}\rho L_{x,2}^\dagger - \frac{1}{2}\{L_{x,2}^\dagger L_{x,2}, \rho\} + L_{x,3}\rho L_{x,3}^\dagger - \frac{1}{2}\{L_{x,3}^\dagger L_{x,3}, \rho\}$ . Then finally solving for the time evolved density matrix we have:

$$\varepsilon(\rho_{ent}(t)) = \frac{1}{4}e^{-4t\gamma} \begin{pmatrix} 1 + e^{4t\gamma} & 0 & 0 & 1 + e^{4t\gamma} \\ 0 & -1 + e^{4t\gamma} & -1 + e^{4t\gamma} & 0 \\ 0 & -1 + e^{4t\gamma} & -1 + e^{4t\gamma} & 0 \\ 1 + e^{4t\gamma} & 0 & 0 & 1 + e^{4t\gamma} \end{pmatrix} \quad (2.44)$$

Then applying unitary quantum teleportation operations to  $\varepsilon(\rho_{ent}(t))$ , we obtain the desired functions for fidelity measurement, they are:

$$F = \frac{1}{16}e^{-4\gamma t - 2i\phi} \left( (1 + e^{2i\phi})^2 \cos(2\theta) (-(e^{4\gamma t} - 1)) + e^{4i\phi} (e^{4\gamma t} - 1) + 2e^{2i\phi} (5e^{4\gamma t} + 3) + e^{4\gamma t} - 1 \right) \quad (2.45)$$

$$F_{avg} = \frac{1}{3} (e^{-4\gamma t} + 2) \quad (2.46)$$

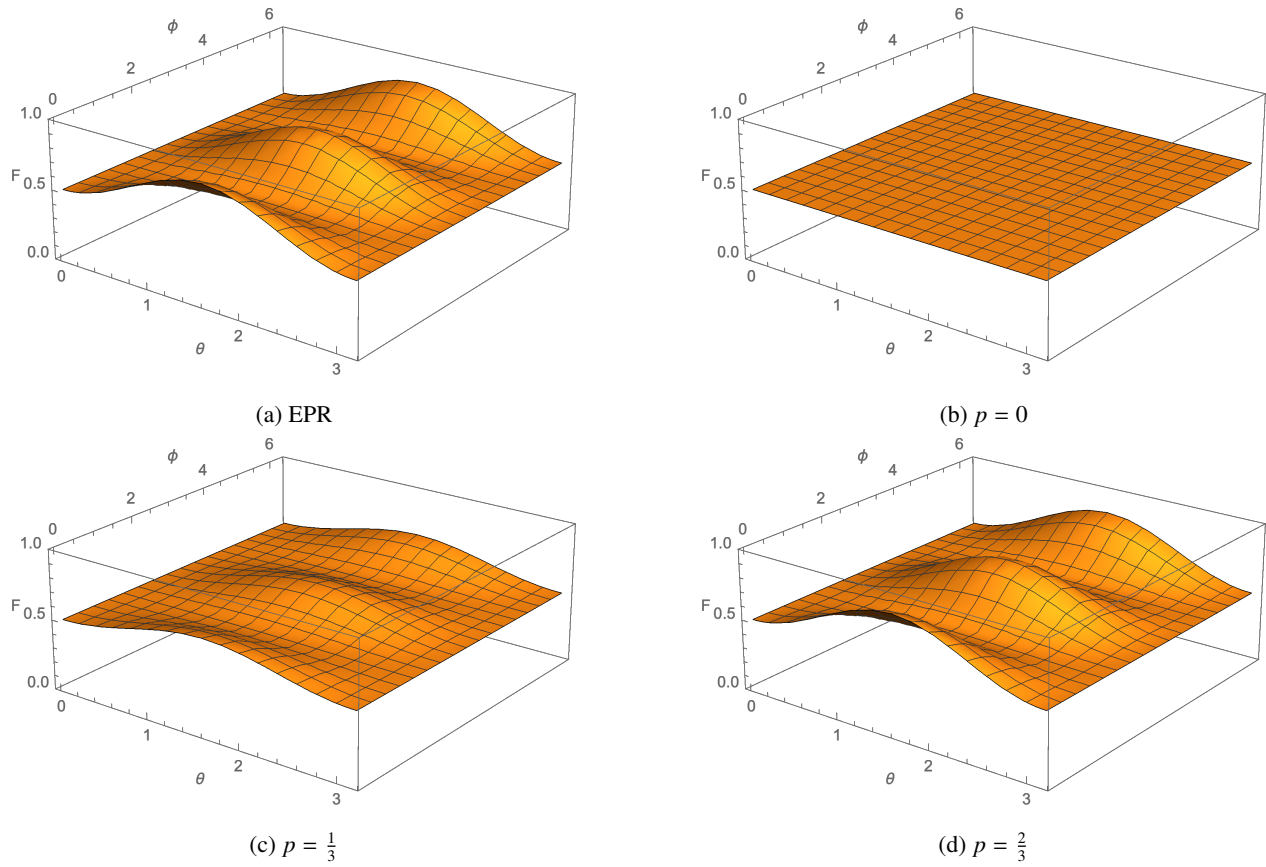


Figure 2.10: The SQT Fidelity vs.  $\theta$  and  $\phi$ , with  $\sigma_x$  noise acting over both qubits. a) Bell's state, b), c), d) Werner states. Values of  $t = 3$ , and  $\gamma = 1$  were fixed for all the plots.

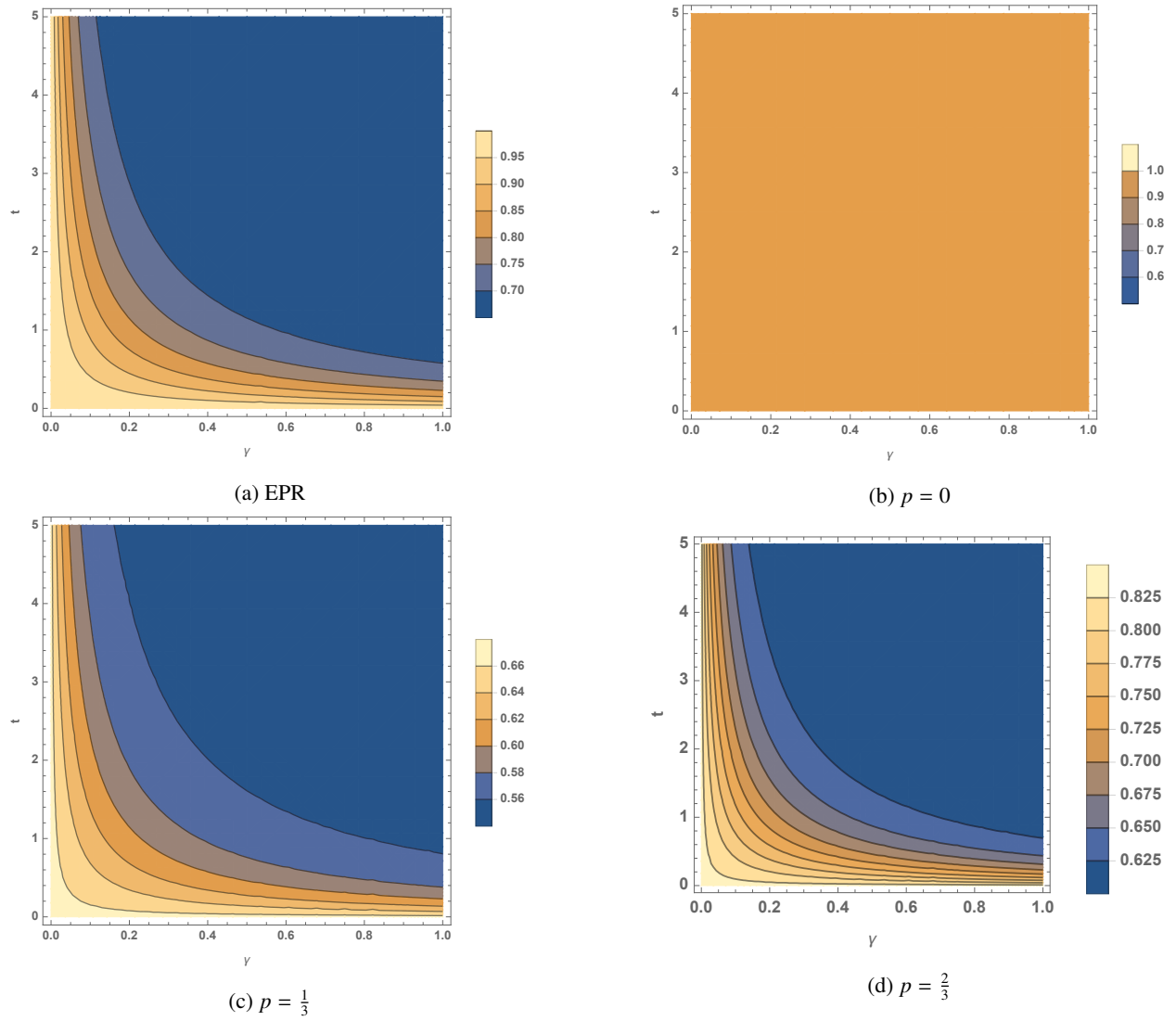


Figure 2.11: Contour plots of  $\gamma$  and  $t$  with noise  $\sigma_z$  acting over both qubits. a) Bell's state, b), c), d) Werner states.

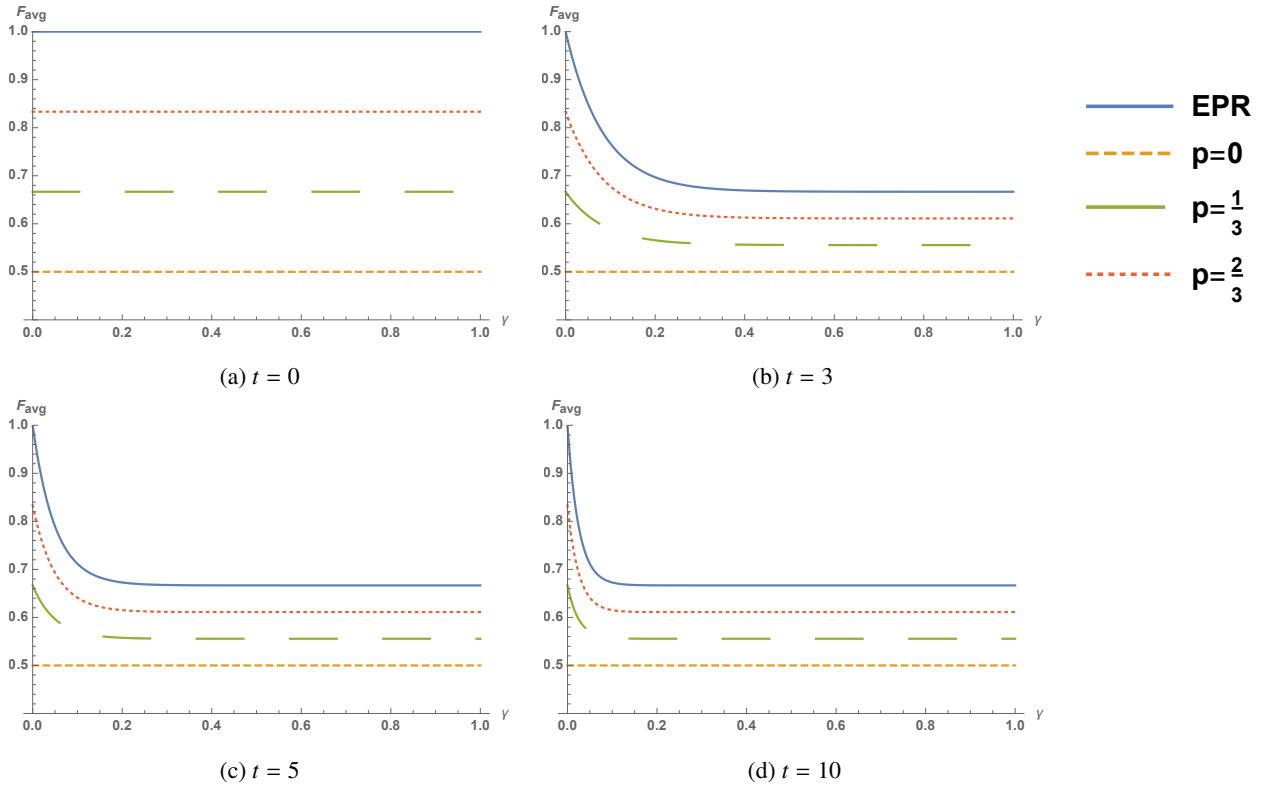


Figure 2.12: The SQT  $F_{avg}$  and  $\gamma$  paramter through time with noise  $\sigma_z$  acting over both qubits. Value of t was fixed for each plot a) t=0, b) t=3, c) t=5, and d) t=10

(c) **Case 2c:** For this last case noise in two different directions is apply. For the qubit 2 z-directional noise is introduced, meanwhile in the other hand for qubit 3 we make use of x-directional noise. In this way we employ the Lindblad operators:  $L_{z,2} = \sqrt{\gamma_{z,2}}\sigma_z^{(2)}$ , and  $L_{x,3} = \sqrt{\gamma_{x,3}}\sigma_x^{(3)}$ , where  $\gamma_{z,2} = \gamma_{x,3}$ . Then introducing them in our Lindblad equation we get:  $\frac{d\rho}{dt} = L_{z,2}\rho L_{z,2}^\dagger - \frac{1}{2}\{L_{z,2}^\dagger L_{z,2}, \rho\} + L_{x,3}\rho L_{x,3}^\dagger - \frac{1}{2}\{L_{x,3}^\dagger L_{x,3}, \rho\}$ , which then lead us to the time evolved expression:

$$\varepsilon(\rho_{em}(t)) = \frac{1}{4}e^{-2t\gamma} \begin{pmatrix} 1 + e^{2t\gamma} & 0 & 0 & e^{-2t\gamma}(1 + e^{2t\gamma}) \\ 0 & -1 + e^{2t\gamma} & e^{-2t\gamma}(-1 + e^{2t\gamma}) & 0 \\ 0 & e^{-2t\gamma}(-1 + e^{2t\gamma}) & -1 + e^{2t\gamma} & 0 \\ e^{-2t\gamma}(1 + e^{2t\gamma}) & 0 & 0 & 1 + e^{2t\gamma} \end{pmatrix} \quad (2.47)$$

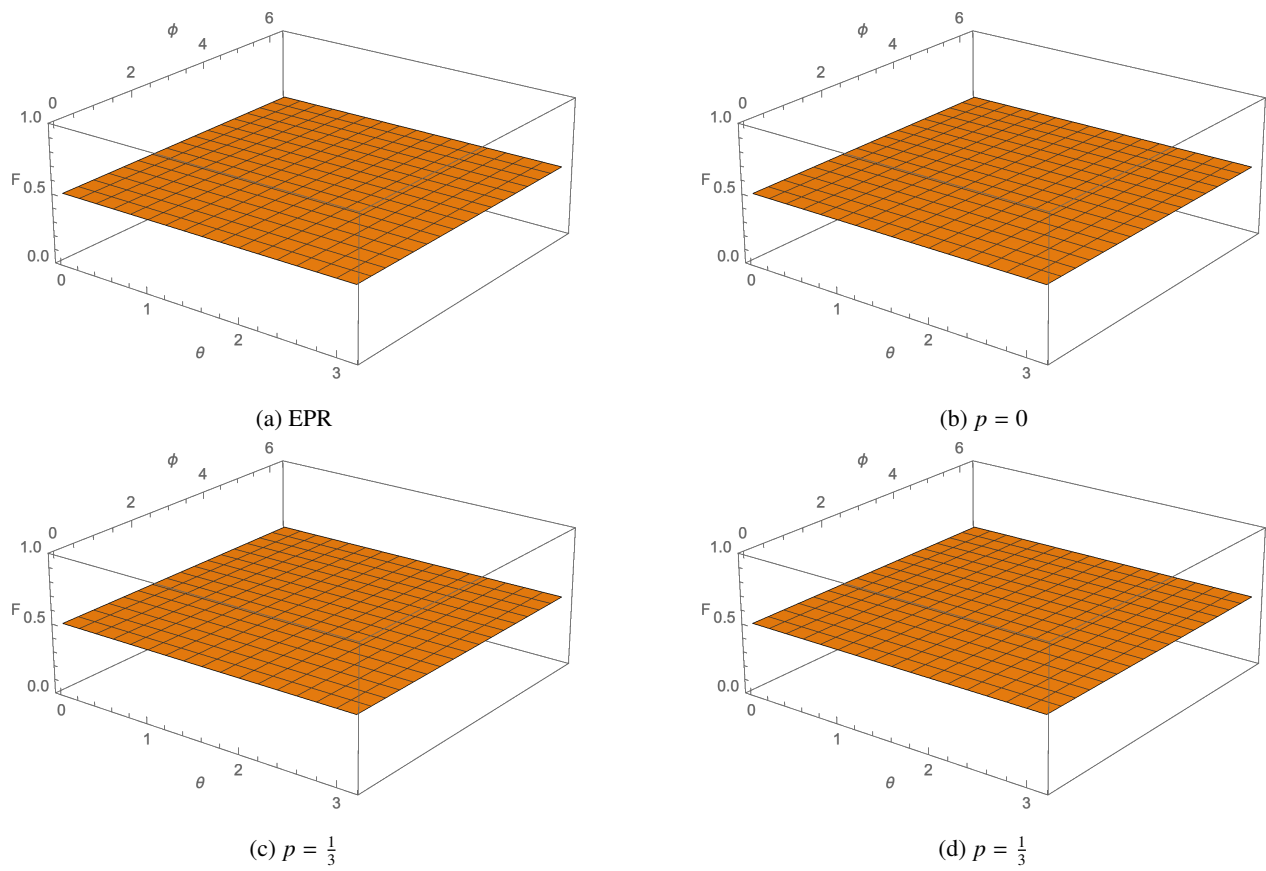


Figure 2.13: The SQT Fidelity vs  $\theta$  and  $\phi$ , with noise  $\sigma_z$  and  $\sigma_x$  acting in second and third qubit. a) Bell's state, b), c), d) Werner states. In each plot values for  $t = 3$ , and  $\gamma = 5$  were fixed.

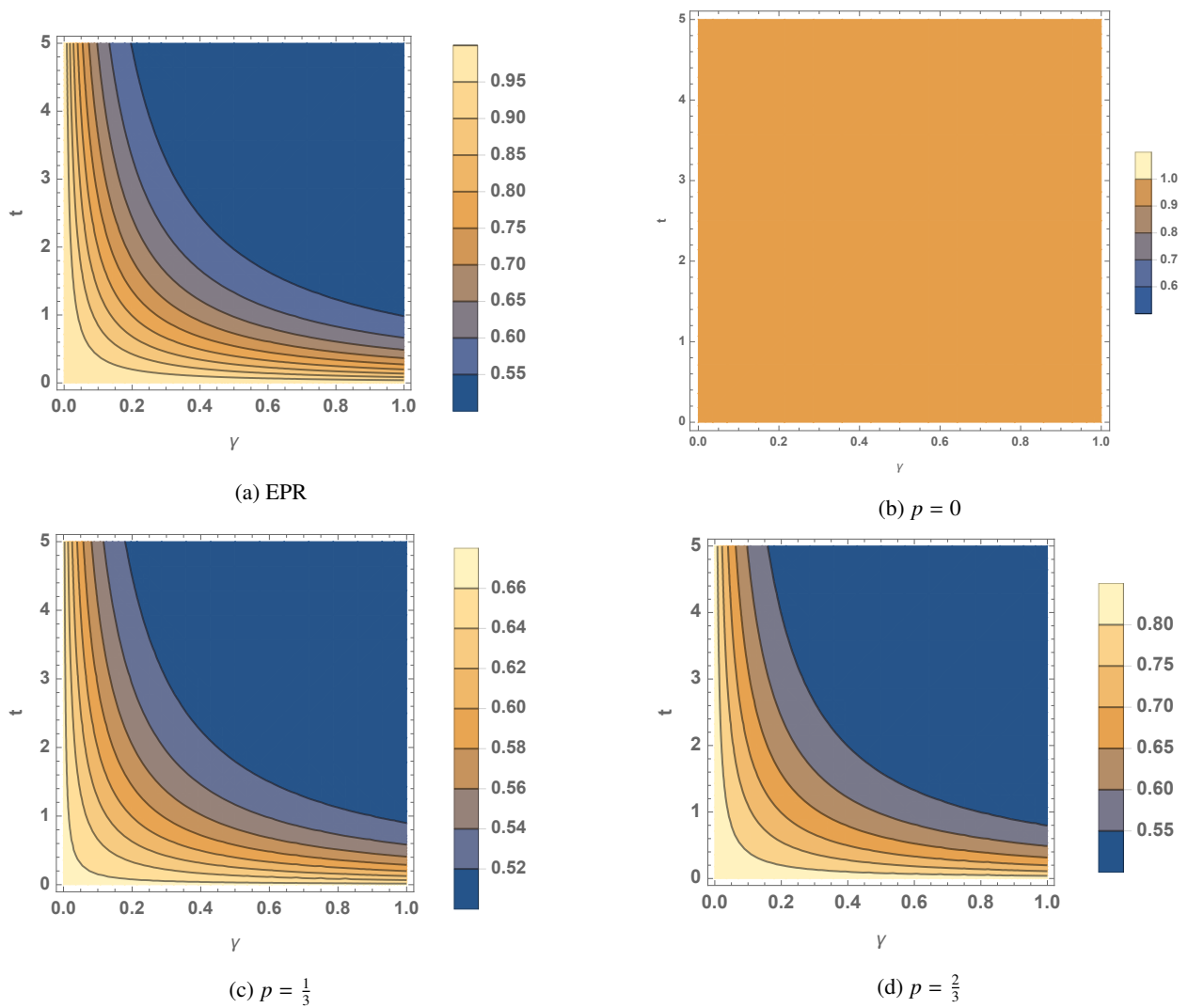


Figure 2.14: Contour plots  $\gamma$  and  $t$ , with noise  $\sigma_z$  and  $\sigma_x$  acting over two qubits. a) Bell's state, b), c), d) Werner states.

In figure 2.14 we can observe the effects of the decoherence caused by the effects of noise acting over two qubits in different  $z$ , and  $x$ -directions. In this case there is not an apparent dependence on the entanglement or angles of the initial state, since in all the graphs all of them show a similar constant behavior. Isotropic noise could cause the complete lost of coherence in the system, drooping the value of fidelity down to its minimum possible value for this case.

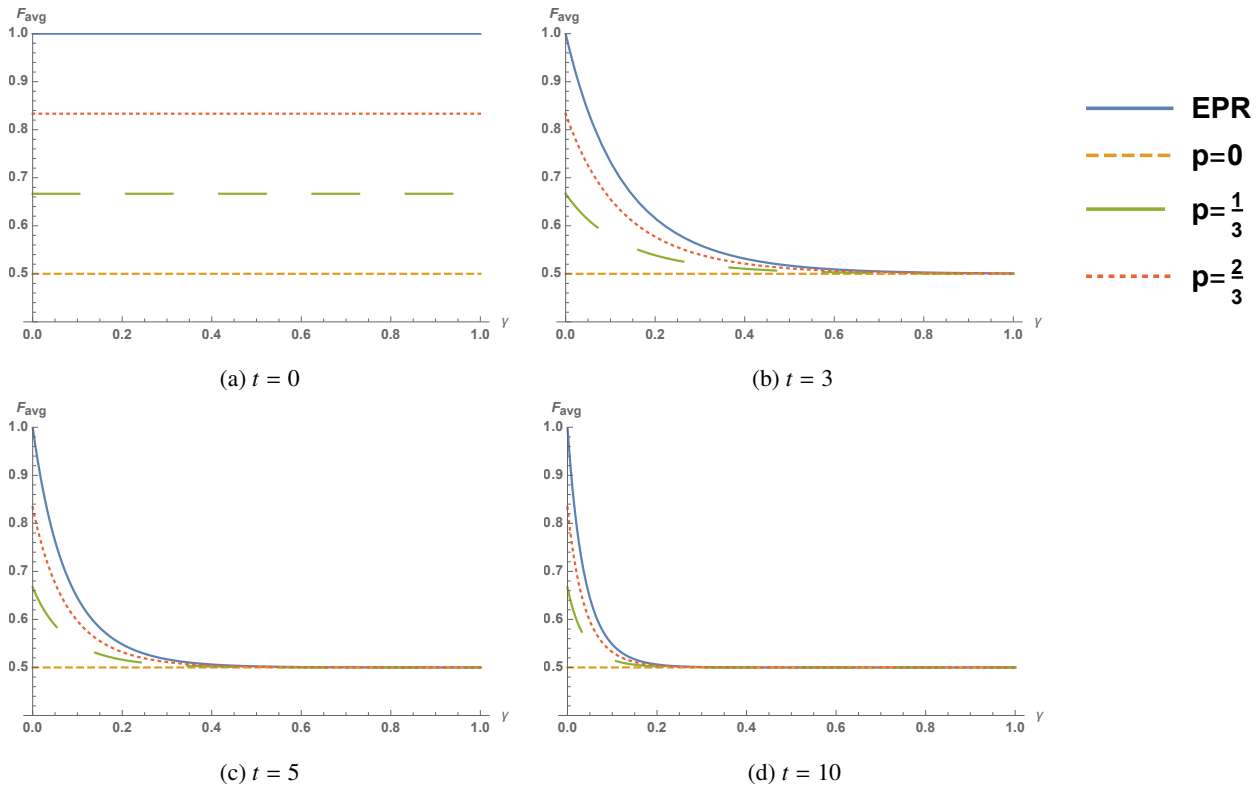


Figure 2.15: The SQT  $F_{avg}$  and  $\gamma$  through time with noise  $\sigma_z$  and  $\sigma_x$  acting over both qubits. For each plot the value for  $t$  was fixed a)  $t = 0$ , b)  $t = 3$ , c)  $t = 5$ , d)  $t = 10$

Contrary to the previous cases in which we observe how for each case they have their own minimal value for the average fidelity, in this case we can observe in figure 2.18, how all the cases converge to the same value as  $t$  and  $\gamma$  parameters increases. Again this behavior could be due to the presence of isotropic noise in the system.

## 2.1.2 Non-Markovian Channel

The non-Markovian channels have been partially studied in [9]. In order to introduce our system to the Non-Markovian regime, we will use the theoretical background use in [10]. Later, we will return to the Master equation. Then accordingly, we can consider our initial state as  $|\Psi^s\rangle = \alpha|HH\rangle + \beta|VV\rangle$ , where  $|H\rangle$  and  $|V\rangle$  represents the vertical and horizontal polarization respectively. In order to represent the environment, transverse momentum of light polarization  $\vec{q} = \{q_x, q_y\}$  is employed, then the environment can be depicted by  $|\psi^e\rangle = \int d\vec{q} f(\vec{q}) |\vec{q}\rangle$  where  $f(\vec{q})$  is the distribution function of the transverse momentum which is normalized  $\int d\vec{q} |f(\vec{q})|^2 = 1$ . It is defined as :

$$|f(q)|^2 = e^{-w_0^2 \cdot q^2} [1 + \cos(2qd_v)], \quad (2.48)$$

where  $w$  is the beam width and  $d_v$  is the tunable parameter.

In order to achieve the desired behavior the initial state must be coupled to the environment such that  $|\psi^{se}\rangle = |\psi^s\rangle \otimes |\psi^e\rangle$ . This coupling generates a unitary transformation over our coupled system which is given by  $\hat{U}(d_c) = \int d\vec{q} e^{iqd_c \sigma_z}$ , equally written:

$$\hat{U}(d_c) = \int dq f(q) |q\rangle \langle q| \otimes (|0\rangle \langle 0| e^{iqd_c} + |1\rangle \langle 1| e^{-iqd_c}). \quad (2.49)$$

his unitary transformation is linked with a spatial displacement parameter  $d_c$ . For the case, dc is considered as the parameter which mediates with temporal evolution. Once the initial state (the Bell state) is transformed by the unitary operator  $\hat{U}(d_c)$ , it evolved state will be:

$$|\psi_{se}(d_c)\rangle = \hat{U}(d_c)|\psi_{se}\rangle = \int dq f(q)(\alpha|00\rangle e^{id_c q} + \beta|11\rangle e^{-id_c q})|q\rangle \quad (2.50)$$

Then we must proceed to find the density matrix for the evolved state which is given by  $\rho_{se}(d_c) = |\psi_{se}(d_c)\rangle\langle\psi_{se}(d_c)|$  and is equivalent to the expression:

$$\begin{aligned} \hat{\rho}^{se}(d_c) = \int dq \int dq' f(q)f^*(q')|q\rangle\langle q'| & (|\alpha|^2|00\rangle\langle 00| + \alpha\beta^*|00\rangle\langle 11|e^{id_c q+id_c q'} \\ & + \beta\alpha^*|11\rangle\langle 00|e^{-id_c q-id_c q'} + |\beta|^2|11\rangle\langle 11|) \end{aligned} \quad (2.51)$$

Since we desire to look the effects of the environment over our system the next step consists in trace out the environment variable from our evolved density matrix leading to:

$$\begin{aligned} \hat{\rho}^s(d_c) = \int d\bar{q}\langle\bar{q}| \int dq \int dq' f(q)f^*(q')\langle\bar{q}|q\rangle\langle q'|\bar{q}\rangle & (|\alpha|^2|00\rangle\langle 00| + \alpha\beta^*|00\rangle\langle 11|e^{id_c q+id_c q'} \\ & + \beta\alpha^*|11\rangle\langle 00|e^{-id_c q-id_c q'} + |\beta|^2|11\rangle\langle 11|) \end{aligned} \quad (2.52)$$

The last expression is only non-vanishing for  $q = q' = \bar{q}$ , then this expression in (2.52) becomes:

$$\hat{\rho}_s(d_c) = \begin{pmatrix} |\alpha|^2 & 0 & 0 & \alpha\beta^*\kappa \\ 0 & 0 & 0 & 0 \\ 0 & 0 & 0 & 0 \\ \beta\alpha^*\kappa^* & 0 & 0 & |\beta|^2 \end{pmatrix}, \quad (2.53)$$

where  $\kappa(d_c) = \int dq |f(q)|^2 e^{2id_c q}$ .

Since dc dependant terms are appearing in the off-diagonal matrix terms, we can conclude they are inducing decoherence of the system. Due to the normalization of the transverse momentum distribution function, it becomes  $|f(q)|^2 = \frac{e^{-\omega^2 \frac{q^2}{2}} (1 - \cos(2d_c q)) \sqrt{w^2}}{e^{-\frac{d_c^2}{\omega^2}} (-1 + e^{-\frac{2d_c^2}{\omega^2}}) \sqrt{2\pi}}$ . Using the last expression for solve  $\kappa(d_c)$  we obtain:

$$\kappa(d_c) = \frac{e^{\frac{d_c(d_c+2d_y)}{\omega^2}} (1 + e^{\frac{4d_c d_y}{\omega^2}} + 2e^{\frac{d_y(2d_c+d_y)}{\omega^2}})}{2(1 + e^{\frac{d_y^2}{\omega^2}})} \quad (2.54)$$

Once expression for  $\kappa$  has been obtained we can now make use of the density matrix for the evolved system  $\hat{\rho}_s(d_c)$ , in order to calculate what is the behavior of the fidelity when it is included in our quantum teleportation protocol. In this way the output density matrix is:

$$\hat{\rho}_{out}(d_c) = Tr_{1,2}\{U_{tel}\hat{\rho}_s(d_c)U_{tel}^\dagger\} = \begin{pmatrix} (|\alpha|^2 + |\beta|^2) \cos^2\left(\frac{\theta}{2}\right) & \frac{1}{2}e^{-i\theta}\kappa \sin(\theta) \\ \frac{1}{2}e^{i\theta}\kappa(\alpha\beta^* + \beta\alpha^*) \sin(\theta) & (|\alpha|^2 + |\beta|^2) \sin^2\left(\frac{\theta}{2}\right) \end{pmatrix} \quad (2.55)$$

$$F(d_c) = \langle\psi^{in}|\hat{\rho}_{out}(d_c)|\psi^{in}\rangle = \frac{1}{4}(\alpha^2 + \beta^2)(3 + \cos(2\theta)) + \alpha\beta\kappa \sin^2(\theta) \quad (2.56)$$

$$F_{avg}(d_c) = \frac{2}{3}(\alpha^2 + \beta^2 + \alpha\beta\kappa) \quad (2.57)$$



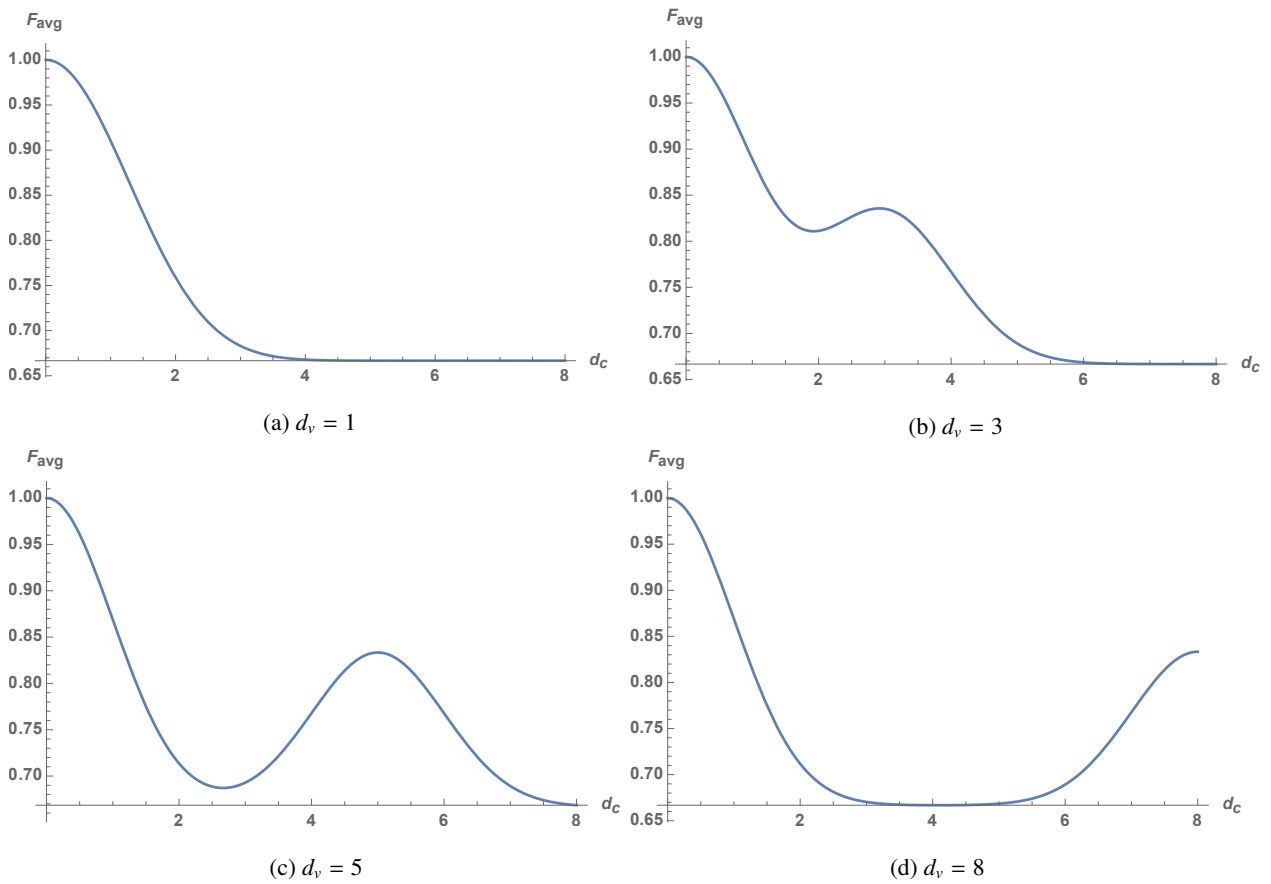


Figure 2.16: The QT fidelity as a function of the coupling strength  $d_c$ . Parameter  $\omega = 2$  has been fixed for all the plots.

Figure 2.16 exhibits the Non-Markovian behavior of the system. As the environment parameter  $d_v$  increases, system starts to recover information from the environment. The coupling strength also needs to increase as  $d_v$  increases in order to observe the Non-Markovian behavior.

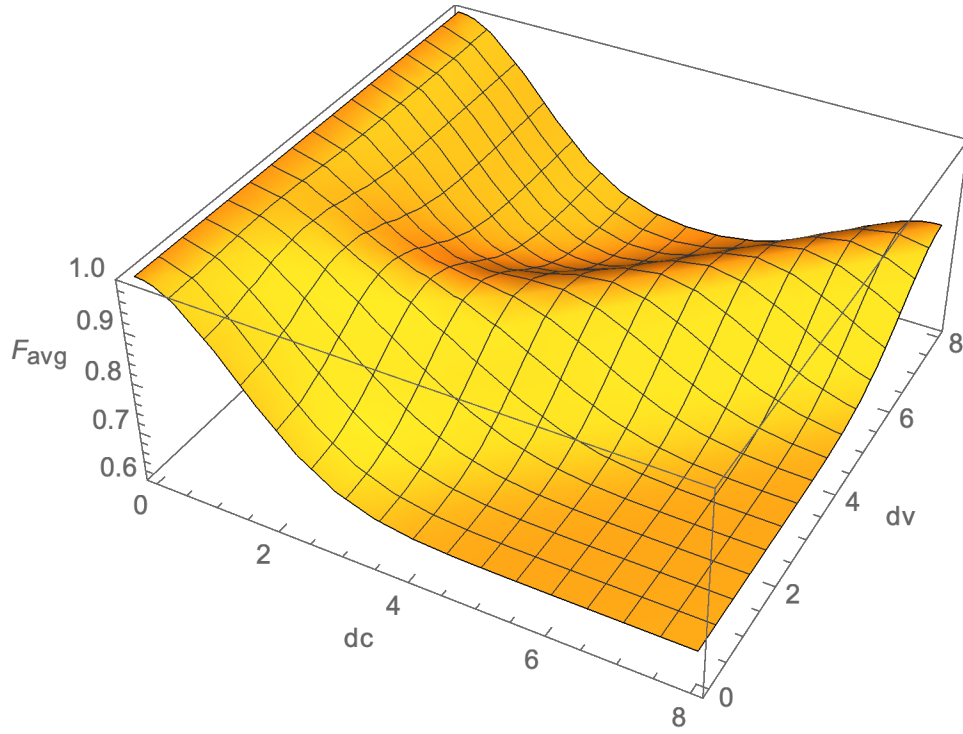


Figure 2.17: The quantum teleportation (QT) fidelity as a function of the coupling strength  $d_c$  and the environment  $d_v$ . The different plots show how is the behavior between  $F_{avg}$ , and  $d_c$  as parameter  $d_v$  increases. The parameter  $\omega = 2$  was fixed

Figure 2.17 shows how in order to observe Non-Markovian behavior it is necessary to maintain a linear relation between the  $d_c$  and  $d_v$  parameters.

In a similar way we can generalize the Non-Markovian case in order to apply to any initial entangled density matrix  $\hat{\rho}_s(0)$ .

Let:

$$\hat{\rho}_s(0) = \begin{pmatrix} P_{00} & P_{01} & P_{02} & P_{03} \\ P_{10} & P_{11} & P_{12} & P_{13} \\ P_{20} & P_{21} & P_{22} & P_{23} \\ P_{30} & P_{31} & P_{32} & P_{33} \end{pmatrix} \quad (2.58)$$

and subsequently our initial state is:  $\hat{\rho} = \hat{\rho}_s(0) \otimes \hat{\rho}_p(0)$ . The momentum initial estate is  $\hat{\rho}_p(0) = |\Phi\rangle\langle\Phi|$  with  $|\Phi\rangle = \int dq f(q)|q\rangle$ . The evolved density matrix then is equal to:

$$\hat{\rho}_s(d_c) = Tr_q\{U(d_c)\hat{\rho}(0)U^\dagger(d_c)\} \quad (2.59)$$

Where  $U(d_c) = \int dq |q\rangle\langle q| e^{iqd_c\hat{\sigma}_z}$ . Then equation (2.59) can be solved similarly to eq. (2.52) obtaining as result:

$$\hat{\rho}_s(d_c) = \begin{pmatrix} P_{00} & P_{01} & P_{02\kappa} & P_{03\kappa} \\ P_{10} & P_{11} & P_{12\kappa} & P_{13\kappa} \\ P_{20\kappa} & P_{21\kappa} & P_{22} & P_{23} \\ P_{30\kappa} & P_{31\kappa} & P_{32} & P_{33} \end{pmatrix} \quad (2.60)$$

Which can be used in order to extend this case using a Werner state in order to construct our initial density matrix, which will be transformed to the evolved density matrix:

$$\hat{\rho}_s(d_c) = \begin{pmatrix} \frac{1+p}{4} & 0 & 0 & \frac{p}{2}\kappa \\ 0 & \frac{1-p}{4} & 0 & 0 \\ 0 & 0 & \frac{1-p}{4} & 0 \\ \frac{p}{2}\kappa & 0 & 0 & \frac{1+p}{4} \end{pmatrix} \quad (2.61)$$

then it can be used to calculate its behavior when it is used in the SQT protocol obtaining the following results:

$$\hat{\rho}_{out}(d_c) = Tr_{1,2}\{U_{tel}\hat{\rho}_s(d_c)U_{tel}^\dagger\} = \begin{pmatrix} \frac{1}{2}(1+p\cos(\theta)) & \frac{1}{4}e^{-i\phi}p\kappa\sin(\theta) \\ \frac{1}{2}e^{i\phi}p\kappa\sin(\theta) & \frac{1}{2}(1-p\cos(\theta)) \end{pmatrix} \quad (2.62)$$

$$F(d_c) = \langle \psi^{in} | \hat{\rho}_{out}(d_c) | \psi^{in} \rangle = \frac{1}{4} (p\cos(2\theta) + 2p\sin^2(\theta)\kappa + p + 2) \quad (2.63)$$

$$F_{avg}(d_c) = \frac{1}{6} (2p\kappa + p + 3) \quad (2.64)$$

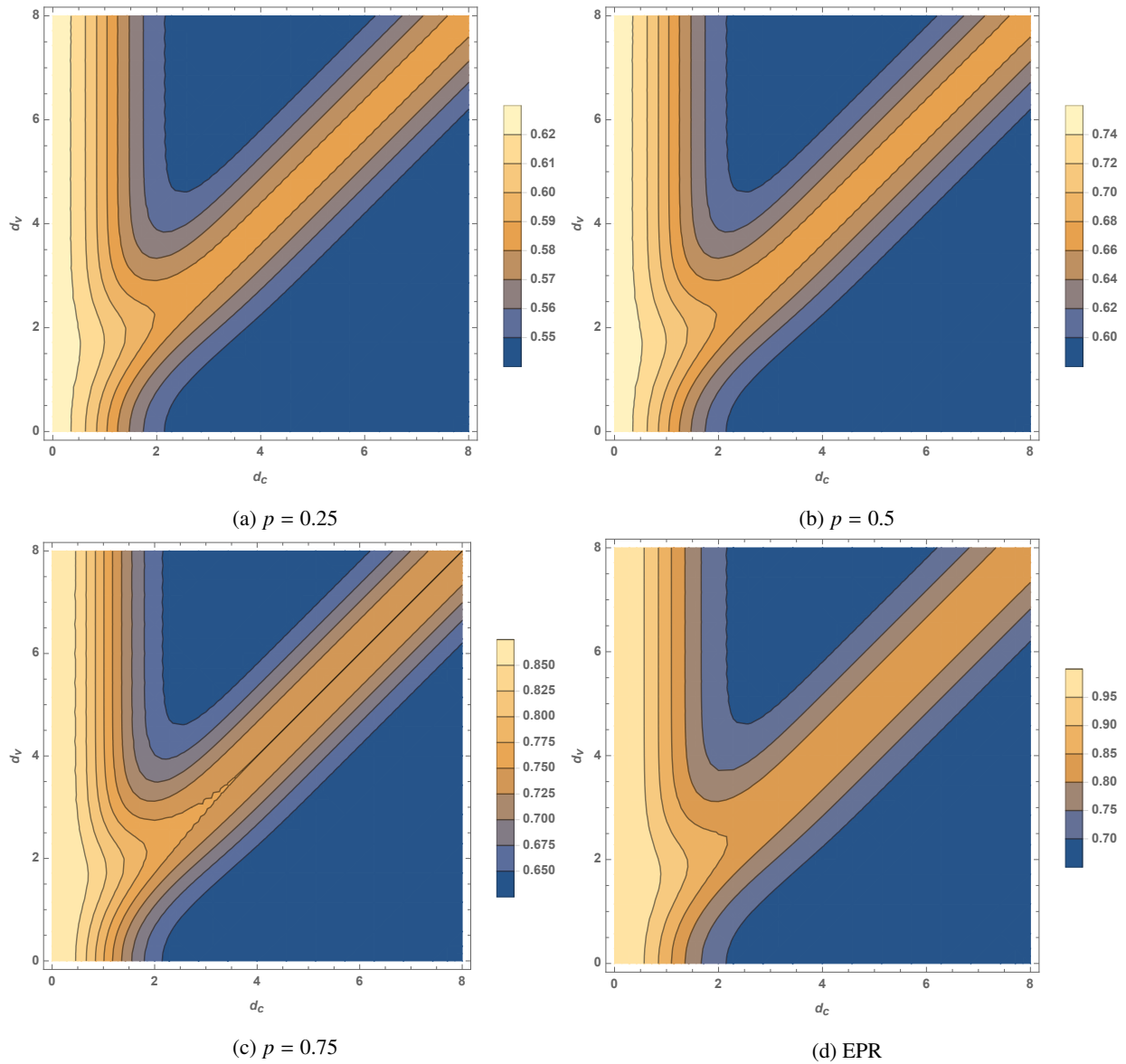


Figure 2.18: Werner state contour plots of SQT  $F_{avg}$  as function of the coupling strength  $d_c$  and  $d_v$  for different values of  $p = a)0.25, b)0.5, c)0.75$ , and Bell's state  $d$ ). All the plots have fixed the value  $\omega = 2$ .

In figure 2.1 we can observe the behavior of the system under Non-Markovian dynamics. Here we can distinguish how a greater level of entanglement of the quantum channel allows us to reach higher values of average fidelity.

### Noisy channels in the Non-Markovian regime: Inserting noise with the Master Equation

In the Markovian regime the master equation allowed us to introduce noise over the quantum entangled channel in our system, in order to understand its effects. For that case the Master equation evolves depending in  $\gamma$  being a time dependent function. In the non-Markovian approach, the behavior of our system depends on the coupling parameter  $d_c$ . In order to understand the effects of noisy channel in the non-Markovian regime it is necessary to find an expression

such that allow us to establish a relation between both  $d_c$  and  $t$ , evolution parameters.

In order to establish the relation we are going to find how  $\gamma(d_c)$ , and  $\kappa(d_c)$  are related. First we need to solve the Lindblad equation, in which we will introduce some noise over our system. If this noise is introduced using the Lindblad operator  $L_{z,2} = \gamma_{z,2}(d_c)\sigma_z^{(2)}$ , our Master equation is given by:  $\frac{d\rho}{dd_c} = L_{z,2}\rho L_{z,2}^\dagger - \frac{1}{2}\{L_{z,2}^\dagger L_{z,2}, \rho\}$ , same which can be written in a simplified form as:

$$\frac{d\hat{\rho}_s}{dd_c} = \gamma(d_c)(\hat{L}_z\hat{\rho}_s\hat{L}_z^\dagger + \hat{\rho}_s) \quad (2.65)$$

And solving L.H.S of (2.65), we find that:

$$\frac{d\hat{\rho}_s}{dd_c} = \begin{pmatrix} 0 & 0 & -2\gamma(d_c)P_{02} & -2\gamma(d_c)P_{03} \\ 0 & 0 & -2\gamma(d_c)P_{12} & -2\gamma(d_c)P_{13} \\ -2\gamma(d_c)P_{20} & -2\gamma(d_c)P_{21} & 0 & 0 \\ -2\gamma(d_c)P_{30} & -2\gamma(d_c)P_{31} & 0 & 0 \end{pmatrix} \quad (2.66)$$

Then we get, eight differential equations with the form:

$$\frac{dP_{m,n}}{dd_c} = -2\gamma(d_c)P_{m,n} \quad (2.67)$$

The same equation that has a solution of the form  $P_{m,n}(d_c) = P_{m,n}(0)e^{-2\int_0^{d_c} dx\gamma(x)}$ . For the second part it is necessary to find the evolved Matrix for the non-Markovian regime. This can be find similarly as was did in (2.60), obtaining as result:

$$\hat{\rho}_s = Tr_q\{\hat{U}(d_c)\hat{\rho}(0)\hat{U}^\dagger(d_c)\} = \begin{pmatrix} P_{00} & P_{01} & P_{02\kappa} & P_{03\kappa} \\ P_{10} & P_{11} & P_{12\kappa} & P_{13\kappa} \\ P_{20\kappa} & P_{21\kappa} & P_{22} & P_{23} \\ P_{30\kappa} & P_{31\kappa} & P_{32} & P_{33} \end{pmatrix} \quad (2.68)$$

Now we can compare between the solution to (2.67) and the evolved matrix  $\hat{\rho}_s$  in (2.68), which results in the relation:

$$\kappa(d_c) = e^{-2\int_0^{d_c} dx\gamma(x)} \quad (2.69)$$

And finally we need to solve last expression for  $\gamma$ , such that:

$$\ln \kappa(d_c) = -2 \int_0^{d_c} dx\gamma(x) \quad (2.70)$$

Then if we derive both sides simultaneously and using Leibnitz integration rule, we arrive to:

$$\frac{1}{\kappa(d_c)} \frac{d\kappa(d_c)}{dd_c} = -2\gamma(d_c) \quad (2.71)$$

which finally lead us to the relation between  $\kappa(d_c)$  and  $\gamma(d_c)$

$$\gamma(d_c) = -\frac{1}{2\kappa(d_c)} \frac{d\kappa(d_c)}{dd_c} \quad (2.72)$$

Now we can make use of this relation in order to prove the effects of noisy channel, within Non-Markovian regime. For this purpose we are going to introduce noise in  $z$ -direction over each of the channel that our system contains. In this way we can establish two possible cases, due to in this case we only have two channels. Nevertheless both cases have a similar behavior as the one that can be observe in the following case:

(a) Case 3a:

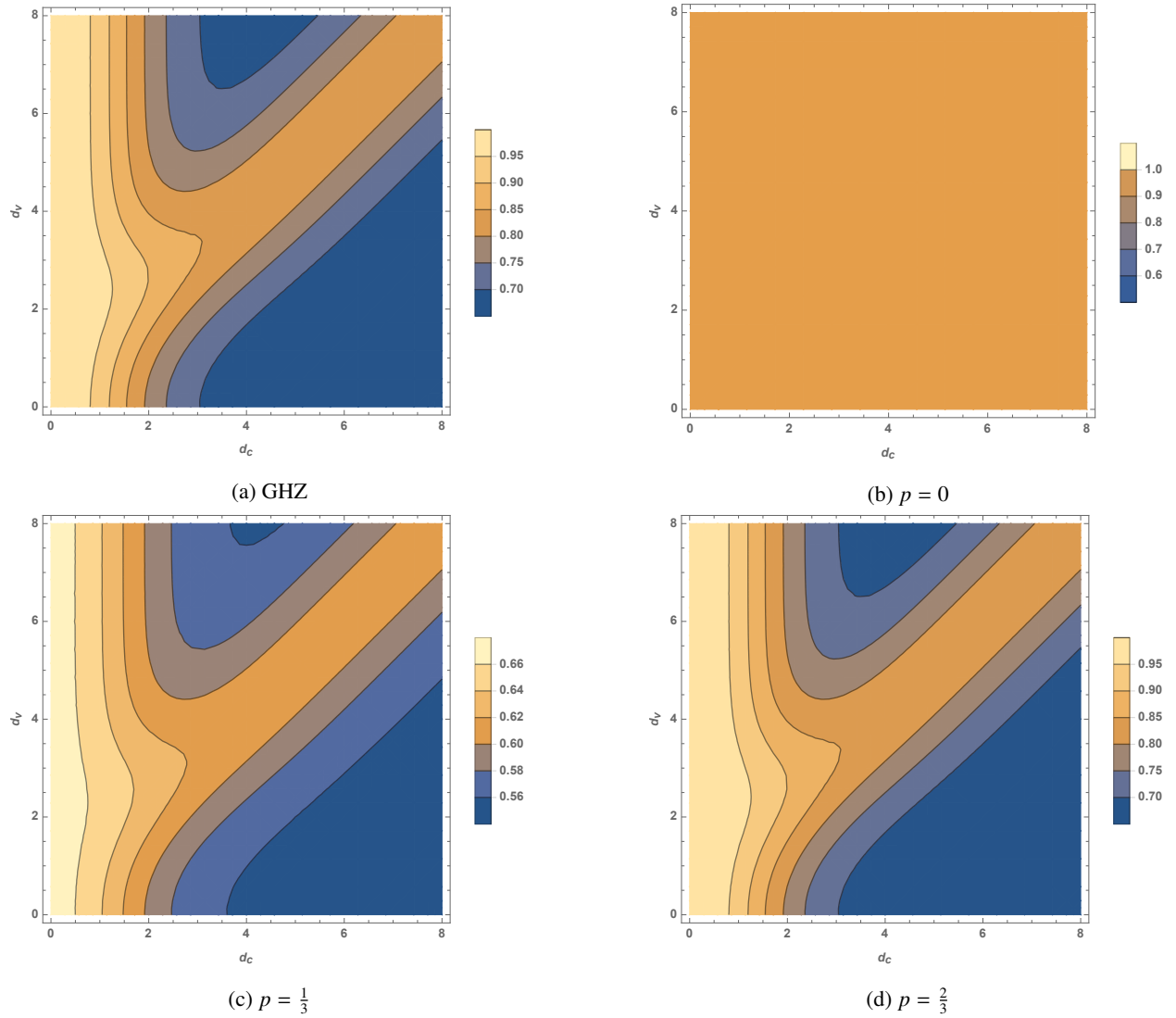


Figure 2.19: Contour plot coupling  $d_c$  parameter and environment  $d_v$ , with noise  $\sigma_z$  acting over one qubit. a) Bell's state, b),c),d) are Werner states. For all the plots the value  $\omega = 2$  has been fixed.

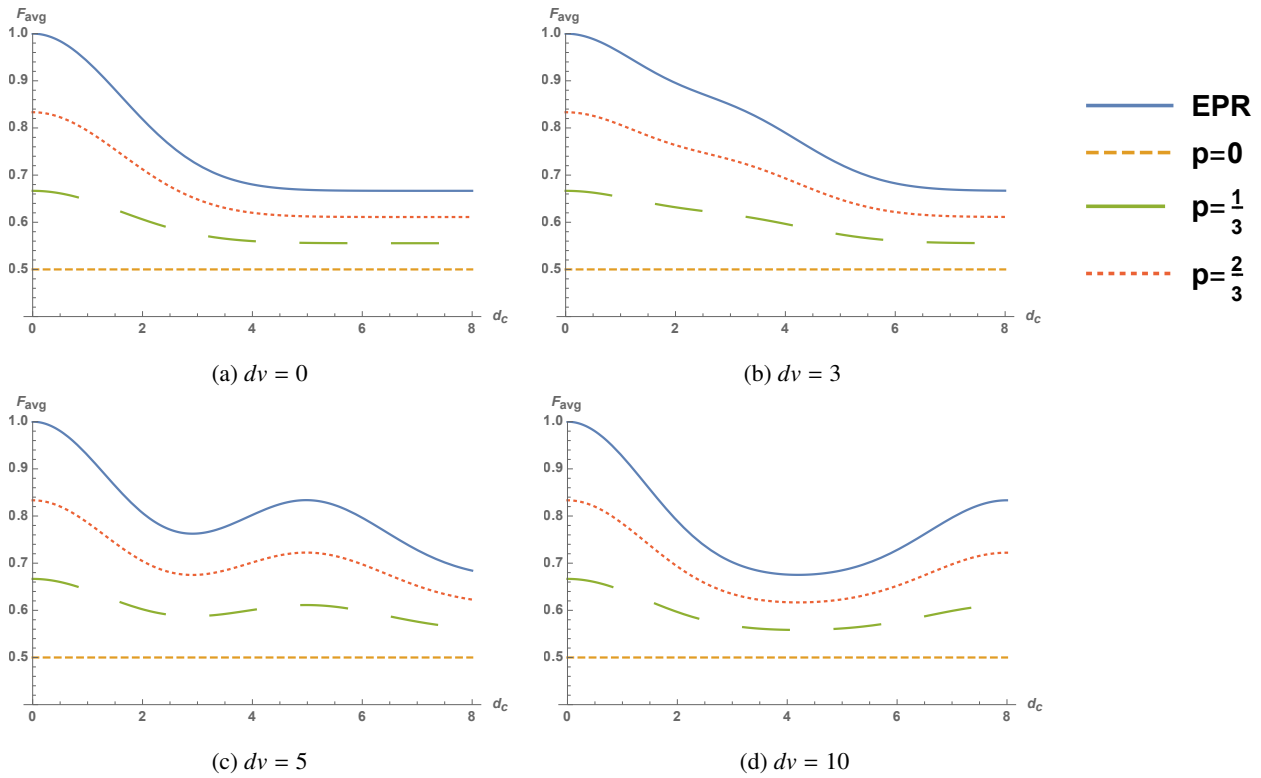


Figure 2.20: The SQT  $F_{avg}$  vs. coupling strength  $d_c$ , with noise  $\sigma_z$  acting over one qubit. The graph shows the behavior as environment parameter  $d_v$  increase.  $F_{avg}$  shows the Non-Markovian behavior just when environment parameter  $d_v$  is large enough, for example in the last plots just c) and d) show to be in the Non-Markovian regime. For all the plots the parameter  $\omega = 2$  was fixed.

## 2.2 Controlled Quantum Teleportation

As was discussed in the first section, controlled quantum teleportation (CQT) is a protocol similar to SQT, but with the main difference that is the participation of a third party (the controller C), which is also related to both A and B, through a tripartite quantum entangled channel. In this case our fully entangled channel (GHZ) is given by:

$$|\psi_{GHZ}\rangle = \frac{1}{\sqrt{2}}(|000\rangle + |111\rangle) \quad (2.73)$$

With the same input state used in SQT described by:

$$|\psi_{in}\rangle = \cos\frac{\theta}{2}|0\rangle + e^{i\phi}\sin\frac{\theta}{2}|1\rangle \quad (2.74)$$

As described in the mathematical models, we can compute two fidelities for the CQT protocol. The first one is the one that is given when there is not present the controller's participation  $F_{NC}$ . The second one, is the fidelity  $F_{CQT}$  when controller's participation is present, and it is in communication with the sender. The communication between Alice and Charlie, allow the correct selection of an appropriate unitary transformation thus fidelity will achieve its maximal value. In order to obtain the results, calculation must be performed numerically in order to find the unitary operation which maximises the Fidelity of CQT. Using these fidelities, we can define the control power P as  $P = F_{CQT} - F_{NC}$ .

The above introduced fidelities are calculated as:

$$F_{NC}(\rho) = \frac{2f_{NC}(\rho) + 1}{3}, \quad \text{where } f_{NC}(\rho) = f(\text{Tr}_C \rho), \quad (2.75)$$

$$F_{CQT}(\rho) = \frac{2f_{CQT}(\rho) + 1}{3}, \quad \text{where } f_{CQT}(\rho) = \max_{U_C} \left[ \sum_{t=0}^1 \langle t|U_C \rho_C U_C^\dagger|t \rangle f(\rho_{SR}^t) \right], \quad (2.76)$$

where

$$\rho_{SR}^t = \frac{\text{Tr}_C[U_C^\dagger|t \rangle \langle t|U_C \otimes_4 \rho U_C^\dagger|t \rangle \langle t|U_C \otimes_4]}{\langle t|U_C \rho_C U_C^\dagger|t \rangle} \quad (2.77)$$

The function  $f$  is the fully entangled fraction [11], which can be obtained for any two-qubit  $\hat{\rho}$  as:

$$f(\hat{\rho}) = \max\{\lambda_1, \lambda_2, \lambda_3, \lambda_4\} \quad (2.78)$$

with  $\{\lambda_i\}_{i=1}^4$  are eigenvalues of the following matrix:

$$M = \text{Re} \begin{pmatrix} \langle \psi_1 | \hat{\rho} | \psi_1 \rangle & \langle \psi_1 | \hat{\rho} | \psi_2 \rangle & \langle \psi_1 | \hat{\rho} | \psi_3 \rangle & \langle \psi_1 | \hat{\rho} | \psi_4 \rangle \\ \langle \psi_2 | \hat{\rho} | \psi_1 \rangle & \langle \psi_2 | \hat{\rho} | \psi_2 \rangle & \langle \psi_2 | \hat{\rho} | \psi_3 \rangle & \langle \psi_2 | \hat{\rho} | \psi_4 \rangle \\ \langle \psi_3 | \hat{\rho} | \psi_1 \rangle & \langle \psi_3 | \hat{\rho} | \psi_2 \rangle & \langle \psi_3 | \hat{\rho} | \psi_3 \rangle & \langle \psi_3 | \hat{\rho} | \psi_4 \rangle \\ \langle \psi_4 | \hat{\rho} | \psi_1 \rangle & \langle \psi_4 | \hat{\rho} | \psi_2 \rangle & \langle \psi_4 | \hat{\rho} | \psi_3 \rangle & \langle \psi_4 | \hat{\rho} | \psi_4 \rangle \end{pmatrix} \quad (2.79)$$

In this section we study CQT protocol using principally three kind of entangled states: GHZ, Werner, and W states. When we evaluate our CQT protocol using these different states we obtain the results described in the next table:

	GHZ	Werner			W
		$p = 0$	$p = \frac{1}{3}$	$p = \frac{2}{3}$	
$F_{NC}(\rho)$	$\frac{2}{3}$	$\frac{1}{2}$	0.5333	0.5833	0.7778
$F_{CQT}(\rho)$	1	$\frac{1}{2}$	0.6	0.75	1
$P(\rho)$	$\frac{1}{3}$	0	0.0667	0.1667	0.2222

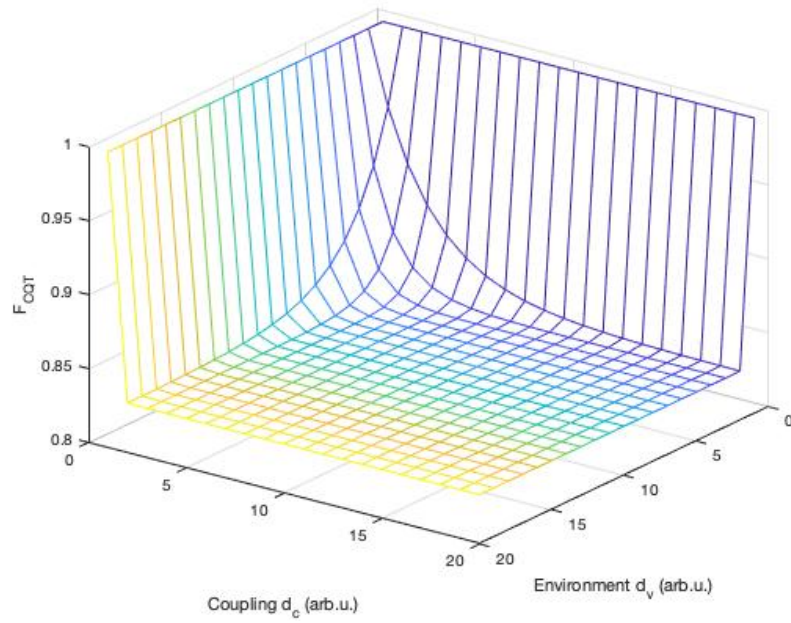
Table 2.1: The different results for controlled fidelity, non-controlled fidelity and control power in terms of the different states for the CQT protocol

Previously, we defined our system as an open one. It is subject to the interactions with the environment. As in the bipartite case these interactions will have consequences over the efficiency of our protocol. In order to study such consequences we need to make use of the Master equation 4 again. This Master equation will allow us to observe the time evolution of our open system, and let us to observe the effects of noise over our quantum channels.

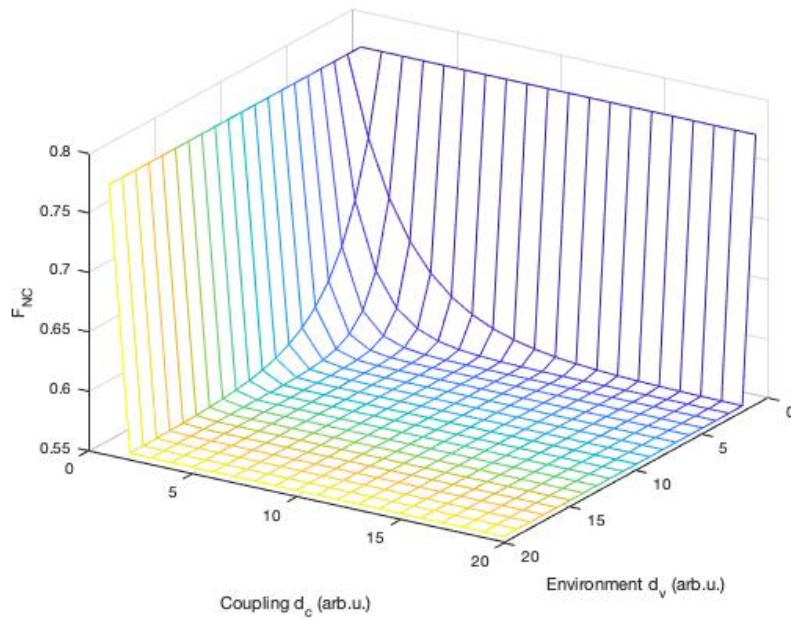
### 2.2.1 Markovian Channel

Here we expect a behavior in which, the system victim of the interaction with environment, will be subject to decoherence as it evolves in time. The obtained results will not only depend on the introduced noise, but also can depend on which type of entangled state is used in the quantum channel. Results are shown in Fig.23.





(a) The CQT fidelity as a function of the coupling strength  $d_c$  and the environment parameter  $d_v$ .



(b) The NC fidelity as a function of the coupling strength  $d_c$  and the environment parameter  $d_v$ .

Figure 2.21: The CQT fidelity, and non-controlled (NC) fidelity as a function of the coupling strength  $d_c$  and environment parameter  $d_v$ , where noise  $\sigma_z$  is acting over one qubit. Parameter  $\omega = 2$  has been fixed for the plots.

Figure 2.21 shows the behavior of CQT fidelity and NC fidelity under the effects on Markovian dynamics. Both presents a behavior very similar to its analogues of Markovian dynamics in SQT. Effects of noise acting over some qubit within the system induces the lost of fidelity.

### 2.2.2 Non-Markovian Channel

For this part we will take into account the bidirectional process in which environment interacting with the system, not only induces its decoherence, but also can have a memory effect. This memory effect is the result of the environment retreating some of the information back to system. Like it was established before, due to the relation between  $\kappa(d_c)$  and  $\gamma(d_c)$  it is also possible to study the effects of noisy channels over the tripartite quantum channel, within the Non-Markovian dynamics. Finally for this part we expect to initially observe some decoherence inducing the lost of fidelity, with a posterior partial recovery of the fidelity. For this purpose noise acting on the z-direction in one channel was studied. In order to observe the effects depending in which channel noise is applied, it was probed channel by channel until complete in the three. According with the result obtained previously we also expect different results depending on the state used in the quantum channel. Due to this consideration CQT for this case was proved with GHZ, Werner, and W states.

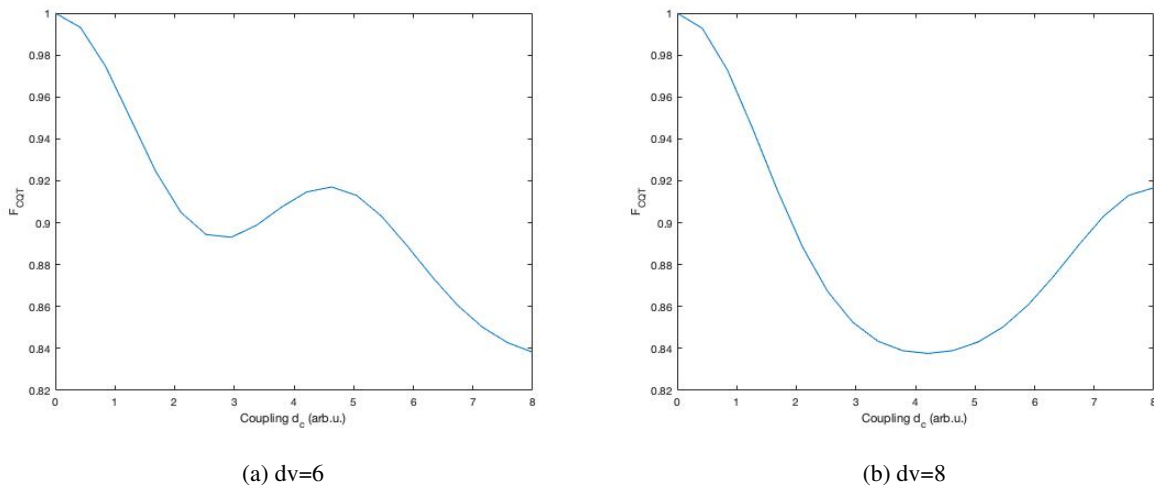


Figure 2.22: The CQT fidelity as a function of the coupling strenght  $d_c$ . Environment parameter is fixed to a)  $d_v = 6$ , and b)  $d_v = 8$ . Parameter  $\omega = 2$  is fixed for both plots.

Figure 2.22 shows how is the behavior CQT fidelity under the presence of Non-Markovian dynamics. As expected the bilateral exchange of information between the environment and the system allows the recovery of information of the system. It means a recovery of the CQT fidelity.

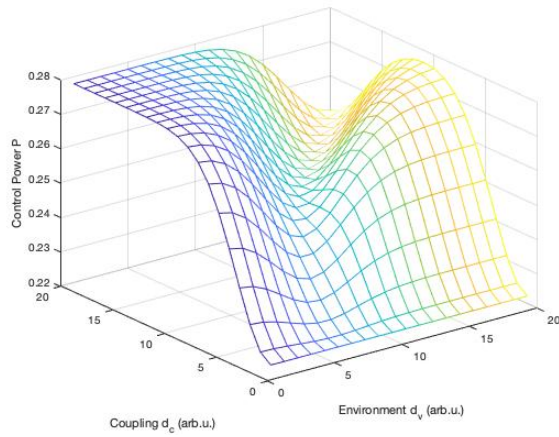
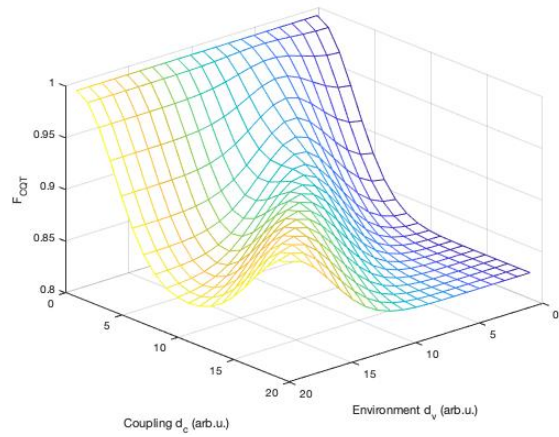
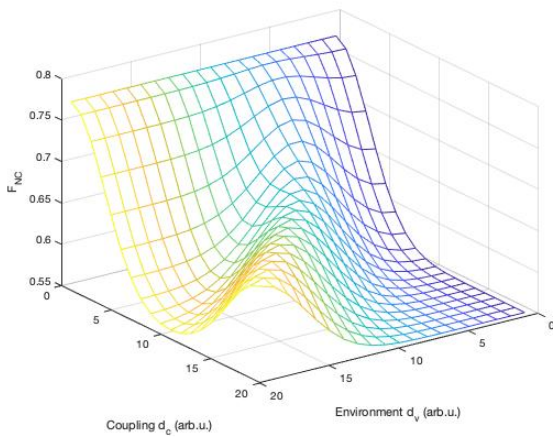
(a) Control Power vs coupling strength  $d_c$ .(b) Controlled fidelity vs. coupling strength  $d_c$ .(c) Non-control fidelity vs. coupling strength  $d_c$ .

Figure 2.23: Results obtained from inserting noise  $\sigma_z$  in the first qubit of the quantum channel with the W state. Parameter  $\omega = 2$  is fixed in all the plots

Figure 2.23 shows the behavior Non-Markovian dynamics under the effects of noise acting in one qubit over  $z$ -direction. In (a) we can observe how not only fidelity is recovered by the system but also its control power.

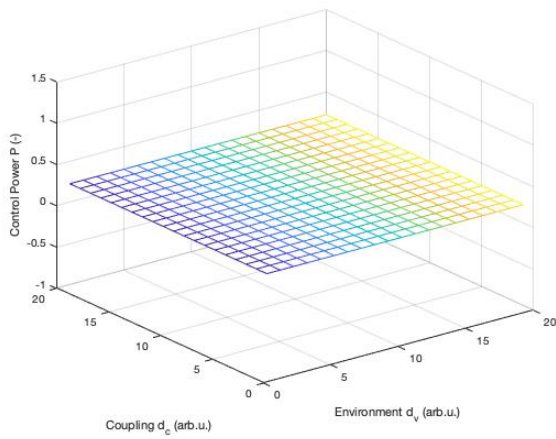
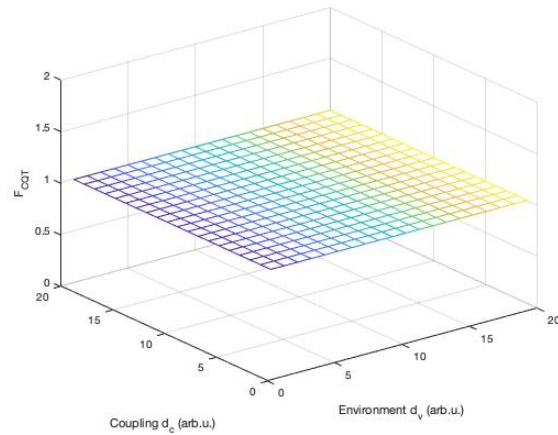
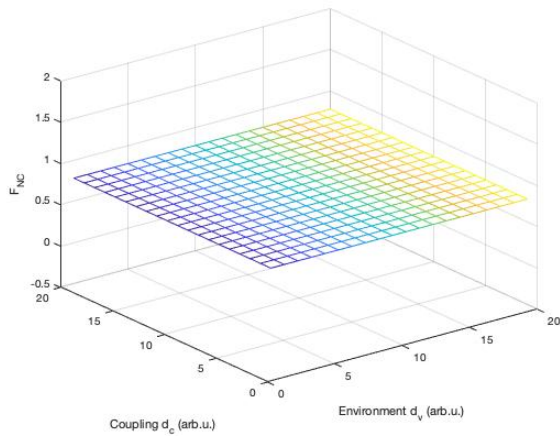
(a) Control Power vs coupling strength  $d_c$  and environment  $d_v$ .(b) Controlled fidelity vs. coupling strength  $d_c$  and environment  $d_v$ .(c) Non-control fidelity vs. coupling strength  $d_c$  and environment  $d_v$ .

Figure 2.24: Results obtained from inserting noise  $\sigma_z$  in the second qubit of the quantum channel with the W state. Parameter  $\omega = 2$  is fixed in all the plots.

Similarly to Fig. (2.24), when some noise is introduced in the Non-Markovian regime making use of the Master equation, and we are using some Greenberger-Horne-Zeilinger (GHZ), or Werner state, their behavior result to be a constant function. In the case of Werner states they are subject also to the parameter  $p$ , which will have also a repercussion in the obtained measurements. As in previous case there is a linear dependence of the Fidelity with the parameter  $p$  which becomes a GHZ state with Fidelity= 1 as  $p \rightarrow 1$ .



## Chapter 3

# Conclusions & Outlook

Use of the quantum teleportation protocol results a great advantage over classical teleportation protocols since the first has a better efficiency than the classical ones, when an unknown quantum state is transmitted. In the study of the bipartite case, as was expected, the standard quantum teleportation (SQT) protocol presents advantage over classical teleportation, reaching the maximum possible fidelity. For the case of Werner states, the resulting fidelity shows a linear dependence on the  $t$  parameter, reaching its minimum for  $p = 0$  and its maximum when  $p = 1$ . Once the noise is introduced in our system decoherence in the system induces the loss of fidelity, despite the decoherence, the minimum average fidelity never goes under the classical limit. The presence of noise in only one of the two channels, causes the same effect, no matter in which direction  $(x,y,z)$  the noise is acting and even on which qubit it is acting. On the other hand, the presence of noise acting simultaneously in more than one qubit certainly leads us to a faster lost of fidelity in comparison to the last case. One interesting effect can be observed in case 2b where noise is introduced in both channels in two different direction, resulting in a loss of the average fidelity that is under the classical upper limit. In the Non-Markovian regime, it was interesting to analyze the behavior that show its effects. In general it behaves as was expected, showing an initial loss of fidelity due to the decoherence and then a partial recovery of the fidelity. We consider that it is important to recall that the environment parameter  $d\nu$  is acting like a switch that allows us to go from Markovian dynamics to Non-Markovian. In the case of the Werner state, we observe a similar behavior but with a fidelity which also gets affected depending on  $p$ .

For the tripartite case, we expect some similar results, but here we start to observe some interesting and surprising effects. When the system is free from noise, behavior in general is exactly the same as for the SQT. Under those conditions the Greenberger-Horne-Zeilinger (GHZ) and W states show a superior efficiency than the classical protocol. The Werner state has also the same behavior, showing a linear dependence of the fidelity depending on the  $p$  parameter. Once we start testing the efficiency of the protocol using noisy channels some peculiarities appear. Contrary to the bipartite case, the GHZs and Werner states do not show a drop in the Fidelity. This behavior tell us that there do not exist any particular dependence of the system on the noise, or even in the non-Markovian regime. The we can assume that fidelity does not get affected by those effects. In the case of the W state we can appreciate the expected behavior. One of the most interesting parts for W states is related with the control power, where we can see certain recovery of the control power where we study its behavior within the non-Markovian dynamics.



# Bibliography

- [1] Nielsen, M. A.; Chuang, I. Quantum computation and quantum information. 2002.
- [2] Bennett, C. H.; Brassard, G.; Crépeau, C.; Jozsa, R.; Peres, A.; Wootters, W. K. Teleporting an unknown quantum state via dual classical and Einstein-Podolsky-Rosen channels. *Physical Review Letters* **1993**, *70*, 1895.
- [3] Bouwmeester, D.; Pan, J.-W.; Mattle, K.; Eibl, M.; Weinfurter, H.; Zeilinger, A. Experimental quantum teleportation. *Nature* **1997**, *390*, 575.
- [4] Karlsson, A.; Bourennane, M. Quantum teleportation using three-particle entanglement. *Physical Review A* **1998**, *58*, 4394.
- [5] Barasiński, A.; ; Arkhipov, I. I.; Svozilík, J. Localizable entanglement as a necessary resource of controlled quantum teleportation. *Scientific Reports* **2018**, *8*, 1–11.
- [6] Barasiński, A.; Černoč, A.; Lemr, K. Demonstration of controlled quantum teleportation for discrete variables on linear optical devices. *Physical Review Letters* **2019**, *122*, 170501.
- [7] Jozsa, R. Fidelity for mixed quantum states. *Journal of Modern Optics* **1994**, *41*, 2315–2323.
- [8] Breuer, H.-P.; Petruccione, F. *The theory of open quantum systems*; Oxford University Press on Demand, 2002.
- [9] Hao, X.; Zhu, S. Enhanced quantum teleportation in non-Markovian environments. *International Journal of Quantum Information* **2012**, *10*, 1250051.
- [10] Urrego, D. F.; Flórez, J.; Svozilík, J.; Nuñez, M.; Valencia, A. Controlling non-Markovian dynamics using a light-based structured environment. *Physical Review A* **2018**, *98*, 053862.
- [11] Grondalski, J.; Etlinger, D.; James, D. The fully entangled fraction as an inclusive measure of entanglement applications. *Physics Letters A* **2002**, *300*, 573–580.





# Abbreviations

**CQT** controlled quantum teleportation v, xii, xiii, 3, 36–38

**EPR** Einstein-Podolsky-Rosen 1, 2, 4, 6

**GHZ** Greenberger-Horne-Zeilinger 3, 41, 43

**NC** non-controlled xii, 38

**QT** quantum teleportation v, xii, 31

**SQT** standard quantum teleportation v, xi, xii, 13, 14, 17–22, 28, 32, 36, 43